



HAL
open science

Local-Group tests of dark-matter concordance cosmology

P. Kroupa, Benoit Famaey, K. S. de Boer, J. Dabringhausen, M. S. Pawlowski, Christian Boily, H. Jerjen, D. Forbes, G. Hensler, M. Metz

► **To cite this version:**

P. Kroupa, Benoit Famaey, K. S. de Boer, J. Dabringhausen, M. S. Pawlowski, et al.. Local-Group tests of dark-matter concordance cosmology. *Astronomy and Astrophysics*, 2010, 523, pp.A32. 10.1051/0004-6361/201014892 . hal-04593550

HAL Id: hal-04593550

<https://hal.science/hal-04593550v1>

Submitted on 30 May 2024

HAL is a multi-disciplinary open access archive for the deposit and dissemination of scientific research documents, whether they are published or not. The documents may come from teaching and research institutions in France or abroad, or from public or private research centers.

L'archive ouverte pluridisciplinaire **HAL**, est destinée au dépôt et à la diffusion de documents scientifiques de niveau recherche, publiés ou non, émanant des établissements d'enseignement et de recherche français ou étrangers, des laboratoires publics ou privés.

Local-Group tests of dark-matter concordance cosmology

Towards a new paradigm for structure formation

P. Kroupa¹, B. Famaey^{1,2,*}, K. S. de Boer¹, J. Dabringhausen¹, M. S. Pawlowski¹, C. M. Boily², H. Jerjen³,
D. Forbes⁴, G. Hensler⁵, and M. Metz^{1,**}

¹ Argelander Institute for Astronomy, University of Bonn, Auf dem Hügel 71, 53121 Bonn, Germany
e-mail: [pavel;deboer;joedab;mpawlow]@astro.uni-bonn.de; manuel.metz@dlr.de

² Observatoire Astronomique, Université de Strasbourg, CNRS UMR 7550, 67000 Strasbourg, France
e-mail: [benoit.famaey;christian.boily]@astro.unistra.fr

³ Research School of Astronomy and Astrophysics, ANU, Mt. Stromlo Observatory, Weston ACT2611, Australia
e-mail: jerjen@mso.anu.edu.au

⁴ Centre for Astrophysics & Supercomputing, Swinburne University, Hawthorn VIC 3122, Australia
e-mail: dforbes@swin.edu.au

⁵ Institute of Astronomy, University of Vienna, Türkenschanzstr. 17, 1180 Vienna, Austria
e-mail: hensler@astro.univie.ac.at

Received 29 April 2010 / Accepted 28 May 2010

ABSTRACT

Predictions of the concordance cosmological model (CCM) of the structures in the environment of large spiral galaxies are compared with observed properties of Local Group galaxies. Five new, most probably irreconcilable problems are uncovered: 1) A wide variety of published CCM models consistently predict some form of relation between dark-matter-mass and luminosity for the Milky Way (MW) satellite galaxies, but none is observed. 2) The mass function of luminous sub-haloes predicted by the CCM contains too few satellites with dark matter (DM) mass $\approx 10^7 M_\odot$ within their innermost 300 pc than in the case of the MW satellites. 3) The Local Group galaxies and data from extragalactic surveys indicate there is a correlation between bulge-mass and the number of luminous satellites that is not predicted by the CCM. 4) The 13 new ultra-faint MW satellites define a disc-of-satellites (DoS) that is virtually identical to the DoS previously found for the 11 classical MW satellites, implying that most of the 24 MW satellites are correlated in phase-space. 5) The occurrence of two MW-type DM halo masses hosting MW-like galaxies is unlikely in the CCM. However, the properties of the Local Group galaxies provide information leading to a solution of the above problems. The DoS and bulge-satellite correlation suggest that dissipational events forming bulges are related to the processes forming phase-space correlated satellite populations. These events are well known to occur since in galaxy encounters energy and angular momentum are expelled in the form of tidal tails, which can fragment to form populations of tidal-dwarf galaxies (TDGs) and associated star clusters. If Local Group satellite galaxies are to be interpreted as TDGs then the substructure predictions of the CCM are internally in conflict. All findings thus suggest that the CCM does not account for the Local Group observations and that therefore existing as well as new viable alternatives have to be further explored. These are discussed and natural solutions for the above problems emerge.

Key words. galaxies: dwarf – galaxies: evolution – gravitation – Local Group – dark matter – cosmology: theory

1. Introduction

Our understanding of the cosmological world relies on two fundamental assumptions: 1) The validity of General Relativity, and 2) conservation of matter since the Big Bang. Both assumptions yield the concordance cosmological model (CCM), according to which an initial inflationary period is followed by (exotic, i.e., non-baryonic) dark-matter (DM) structures forming and then accreting baryonic matter, which fuels star formation in the emerging galaxies, and according to which dark energy (represented by a cosmological constant Λ) drives the acceleration of the Universe at a later epoch. One important way to test assumption (1) is to compare the phase-space properties of the nearest galaxies with the expectations of the CCM. These tests are the focus of the present contribution.

The possibility of the existence of DM was considered more than 85 years ago (Einstein 1921; Oort 1932; Zwicky 1933),

and has been under heavy theoretical and experimental scrutiny (Bertone et al. 2005) since the discovery of non-Keplerian galactic rotation curves by Rubin & Ford (1970) and their verification and full establishment by Bosma (1981). The existence of DM is popularly assumed because it complies with the General Theory of Relativity, and therefore Newtonian dynamics, in the weak-field limit. Newtonian dynamics is the simplest form of gravitational dynamics given that the equations of motion are linear in the potential, and is thus readily accessible to numerical simulations of cosmic evolution, upon which the concordance scenario of structure formation is based (Blumenthal et al. 1984).

The concordance bottom-up scenario of structure formation involving the repeated accretion of clumps of cold dark matter (CDM) is assumed to operate throughout the Universe on all scales. CDM particles with masses of order of about 100 GeV are the preferred candidates to account for constraints placed on the matter density, Ω_M , of thermal relics with realistic cross-sections (see, e.g., Eq. (28) of Bertone et al. 2005). For lighter particle candidates, the damping scale becomes too large: for instance, a hot DM (HDM) particle candidate ($m_{\text{HDM}} \approx \text{few eV}$)

* Alexander von Humboldt Fellow.

** Now at the Deutsches Zentrum für Luft- und Raumfahrt, Königswinterer Str. 522-524, 53227 Bonn, Germany.

would have a free-streaming length of ≈ 100 Mpc leading to too little power at the small-scale end of the matter power spectrum. The existence of galaxies at redshift $z \approx 6$ implies that the coherence scale should have been smaller than 100 kpc or so, meaning that warm DM (WDM) particles with mass $m_{\text{WDM}} \approx 1\text{--}10$ keV are close to being ruled out (Peacock 2003).

CDM is a concept that, together with the cosmological constant (Λ), has been motivated primarily by large-scale observations of, e.g., the cosmic microwave background (CMB) radiation (WMAP, Spergel et al. 2007; Komatsu et al. 2009), the accelerating universe (Riess et al. 1998; Perlmutter et al. 1999), or the power spectrum of density perturbations from the SDSS (Tegmark et al. 2004) and the 2dF galaxy redshift survey (Cole et al. 2005), all of which serve as empirical benchmarks for calibrating and constraining theoretical scenarios and cosmological models. This concordance Λ CDM model is consistent with observations on the Gpc to Mpc scales (Reyes et al. 2010), but it implies that the Universe evolves towards an infinite energy content¹ due to the creation of vacuum energy from dark-energy-driven accelerated expansion (e.g. Peacock 1999)². Less problematically perhaps, but nevertheless noteworthy, the DM particle cannot be contained in the Standard Model of particle physics without implying a significant revision of particle physics (e.g. Peacock 1999). Strong evidence for the existence of DM has been suggested by the observations of the interacting galaxy-cluster pair 1E0657-56 (the “Bullet cluster”, Clowe et al. 2006). The velocity of the sub-cluster relative to the large cluster has since been calculated to be about 3000 km s^{-1} so that the observed morphology can arise (Mastropietro & Burkert 2008). But according to Angus & McGaugh (2008) and Lee & Komatsu (2010), such high velocities between a sub-cluster and a main galaxy cluster are virtually excluded in the CCM. Near the centre of lens-galaxies, the observed delay times between the multiple images of strongly lensed background sources cannot be understood if the galaxy has a standard (NFW or isothermal) DM content and if, at the same time, the Hubble constant has a classical value of $70 \text{ km s}^{-1} \text{ Mpc}^{-1}$: the solution is either to decrease the Hubble constant (in disagreement with other observations), or to consider the known baryonic matter (with constant mass-to-light ratio) as the one and only source of the lensing (Kochanek & Schechter 2004). On Local Volume scales (within about 8 Mpc), it has been pointed out that the Local Void contains far fewer dwarf galaxies than expected if the CCM were true. At the same time, there are too many large galaxies in the less crowded parts such that the arrangement of massive galaxies in the Local Volume is less than 1 per cent likely in the CCM (Peebles & Nusser 2010).

This discussion highlights that there are important unsolved issues in the CCM. This clearly means that substantial effort is required to understand the problems, to perhaps distill additional clues from the data that can provide solutions, and to improve the theory.

Galaxy formation and evolution is a process that happens on scales much smaller than 1 Mpc. Ironically, a major limitation of our ability to develop a physically consistent model of

how galaxies evolved out of the dark comes from incomplete knowledge of the Local Group, in particular from the lack of understanding of the structure and distribution of dwarf satellite galaxies. But, over the past few years, a steady flow of new results from nearby galaxies including the Milky Way (MW) and the improving numerical resolution of computational studies of galaxy formation have allowed ever more rigorous tests of the CCM.

According to the DM hypothesis, galaxies must have assembled by means of accretion and numerous mergers of smaller DM halos. Therefore, galaxies such as the MW should be swarmed by hundreds to thousands of these halos (Moore et al. 1999a; Diemand et al. 2008), whereby the number of sub-halos is smaller in WDM than in CDM models (Knebe et al. 2008). Furthermore, the triaxial nature of the flow of matter at formation would make it impossible to destroy halo substructure by violent relaxation (Boily et al. 2004). These sub-halos should be distributed approximately isotropically about their host, and have a mass function such that the number of sub-halos in the mass interval $M_{\text{vir}}, M_{\text{vir}} + dM_{\text{vir}}$ is approximately $dN \propto M_{\text{vir}}^{-1.9} dM_{\text{vir}}$ (Gao et al. 2004).

In contrast to this expectation, only a few dozen shining satellites have been found around both the MW and Andromeda (M31), while the next largest disc galaxy in the Local Group, M33, has no known satellites. The MW hosts the 11 “classical” (brightest) satellites, while 13 additional “new” and mostly ultra-faint satellite galaxies have been discovered in the past 15 years primarily by the Sloan Digital Sky Survey (SDSS)³. While the MW satellites are distributed highly anisotropically (e.g. Klimentowski et al. 2010), observations of the internal kinematics (velocity dispersion) of the satellites suggest they are the most DM dominated galaxies known (e.g. Fig. 15 in Simon & Geha 2007). That is, the velocity dispersions of their stars seem to be defined by an unseen mass component: the stars are moving faster than can be accounted for by their luminous matter. The known satellites may therefore be the luminous “tip of the iceberg” of the vast number of dark sub-halos orbiting major galaxies such as the MW.

Much theoretical effort has been invested in solving the problem that the number of luminous satellites is so much smaller than the number of DM-halos predicted by the currently favoured concordance Λ CDM hypothesis: stellar feedback and heating processes limit baryonic growth, re-ionisation stops low-mass DM halos from accreting sufficient gas to form stars, and tidal forces from the host halo limit growth of the DM sub-halos and lead to truncation of DM sub-halos (Dekel & Silk 1986; Dekel & Woo 2003; Macciò et al. 2009; Koposov et al. 2009; Okamoto & Frenk 2009; Kirby et al. 2009; Shaya et al. 2009; Busha et al. 2010; Macciò et al. 2010). This impressive and important theoretical effort has led to a detailed quantification of the DM-mass-luminosity relation of MW satellite galaxies. Moreover, the discovery of new (ultra-faint) dSph satellites around the MW suggests the validity of the “tip of the iceberg” notion. These lines of reasoning have generally led to the understanding that within the Λ CDM cosmology, no serious small-scale issues are apparent (e.g. Tollerud et al. 2008; Primack 2009).

¹ One may refer to this issue as the “cosmological energy catastrophe” in allusion to the black body UV catastrophe, which led Max Planck to heuristically introduce an auxiliary (= *Hilfsgröße* in German) number h , to reproduce the black body spectrum.

² Energy conservation is a problematical issue in General Relativity (GR). The stress-momentum-energy tensor is a pseudo tensor and so is not invariant under a transformation to a different coordinate system and back. This may perhaps be considered to indicate that GR may not be complete.

³ For convenience, the 11 brightest satellite galaxies are here referred to as the “classical” satellites because these were known before the SDSS era. These include the LMC and the SMC with the others being dwarf spheroidals. The other, more recently discovered satellites are fainter than the faintest “classical” satellites (UMi and Draco), and these are called the “new” or the “ultra-faint” satellites or dwarfs (see Table 2).

In this contribution we test whether the CCM can be viewed as a correct description of the Universe by studying generic properties of the Local Group⁴, which is a typical environment for galaxies – the Local Group properties *must* conform to the CCM if it is to be valid universally. To test this hypothesis, we critically examine state-of-the-art models calculated within the CDM and WDM framework by a number of independent research groups developed to explain the properties of the faint satellite galaxies, by comparing them with the following observations: the mass-luminosity relation for dSph satellites of the Milky Way (Sect. 2); the mass-distribution of luminous-satellite halomasses (Sect. 3); and the observed relation between the bulge mass of the host galaxy and the number of satellites (Sect. 4). The question of whether the Disc-of-Satellites (DoS) exists, and if in fact the latest MW satellite discoveries follow the DoS, or whether the existence of the DoS is challenged by them, is addressed in Sect. 5. In Sect. 5, the observed invariance of late-type baryonic galaxies is also discussed in the context of the Local Group. In these sections it emerges that the CCM has problems relating to the observed data. In Sect. 6 the problems are interpreted as clues to a possible solution of the origin of the satellite galaxies. The implications of testing the CCM on the Local Group for gravitational theories are also discussed. Conclusions regarding the consequences of this are drawn in Sect. 7.

2. The satellite mass – luminosity relation (problem 1)

Our understanding of the physical world relies on some fundamental physical principles. Among them is the conservation of energy. This concept implies that it is increasingly more difficult to unbind sub-components from a host system with increasing host binding energy.

Within the DM hypothesis, the principle of energy conservation therefore governs how DM potentials fill-up with matter. There are two broadly different physical models exploring the consequences of this, namely models of DM halos based on internal energy sources (mostly stellar feedback), and models based on external energy input (mostly ionisation radiation). In the following, the observational mass-luminosity data for the known satellite galaxies are discussed, and the data are then compared to the theoretical results that are calculated within the CCM.

2.1. The observational data

Based on high quality measurements of individual stellar line-of-sight velocities in the satellite galaxies, [Strigari et al. \(2008\)](#) (hereinafter S08) calculate dynamical masses, $M_{0.3 \text{ kpc}}$, within the inner 0.3 kpc of 18 MW dSph satellite galaxies over a wide range of luminosities ($10^3 \lesssim L/L_\odot \lesssim 10^7$). The LMC and SMC are excluded, as is Sagittarius because it is currently experiencing significant tidal disturbance. S08 significantly improve the previous works by using larger stellar data sets and more than double the number of dwarf galaxies, and by applying more detailed mass modelling. Their results confirm the earlier suggestion by [Mateo et al. \(1993\)](#), [Mateo \(1998\)](#), [Gilmore et al. \(2007\)](#), and [Peñarrubia et al. \(2008\)](#) that the satellites share a common DM mass scale of about $10^7 M_\odot$, “and conclusively establish” (S08) this common mass scale.

⁴ Useful reviews of the Local Group are provided by [Mateo \(1998\)](#) and [van den Bergh \(1999\)](#).

Table 1. The slope of the DM-mass-luminosity relation of dSph satellite galaxies.

data	κ	Radius [pc]	M_0 [$10^7 M_\odot$]
Observational:			
1	$+0.02 \pm 0.03$	300	1.02 ± 0.39
2	$+0.02 \pm 0.03$	300	1.01 ± 0.40
3	$+0.01 \pm 0.03$	300	1.09 ± 0.44
*4	-0.03 ± 0.05	600	6.9 ± 4.9
DM Models:			
A: feedback	0.21	300	–
B1: re-ionisation, SPS	0.15 ± 0.02	300	0.24 ± 0.06
B2: re-ionisation	0.17 ± 0.01	300	0.18 ± 0.02
C: SAM	0.42 ± 0.02	300	2.0 ± 0.9
*D: Aq-D-HR	0.17 ± 0.02	600	0.41 ± 0.14
E1: 1keV(WDM)	0.23 ± 0.04	300	0.069 ± 0.045
E2: 5keV(WDM)	0.12 ± 0.02	300	0.43 ± 0.081
F: Aq-infall	0.13 ± 0.01	300	0.32 ± 0.022

Notes. Fitted parameters for Eq. (1).

Fits to $\kappa = 0.35/\eta$: data 1–4 are observational values, data A–F are models (see Sect. 2).

1: our fit to S08 (who give central 300 pc masses, 18 satellites, their Fig. 1). 2: our fit to S08 without Seg.1 (faintest satellite, i.e. 17 satellites, their Fig. 1). 3: our fit to S08 without Seg.1 and without Hercules (i.e. 16 satellites, their Fig. 1). 4: our fit to the observational data plotted by [Okamoto & Frenk \(2009\)](#) (who give central 600 pc masses, only 8 satellites, their Fig. 1). A: [Dekel & Silk \(1986\)](#); [Dekel & Woo \(2003\)](#), stellar feedback (Eq. (5)). B1: our fit to [Busha et al. \(2010\)](#), their SPS model. B2: our fit to [Busha et al. \(2010\)](#), inhomogeneous re-ionisation model. C: our fit to [Macciò et al. \(2010\)](#), semi-analytical modelling (SAM), fit is for $L_V > 3 \times 10^5 L_{V,\odot}$. D: our fit to [Okamoto & Frenk \(2009\)](#) (Aq-D-HR). E1: our fit to the 1 keV WDM model of [Macciò & Fontanot \(2010\)](#). E2: our fit to the 5 keV WDM model of [Macciò & Fontanot \(2010\)](#). F: our fit to the Aquarius sub-halo-infall models of [Cooper et al. \(2010\)](#). *: the entries with an asterisk are for the central 600 pc radius region.

The finding of S08 can be quantified by writing

$$\log_{10} M_{0.3 \text{ kpc}} = \log_{10} M_0 + \kappa \log_{10} L, \quad (1)$$

and by evaluating the slope, κ , and the scaling, M_0 . S08 derive $\kappa = 0.03 \pm 0.03$ and $M_0 \approx 10^7 M_\odot$. Using the Dexter Java application of [Demleitner et al. \(2001\)](#), a nonlinear, asymmetric error weighted least squares fit to the S08 measurements reproduces the common mass and slope found by S08, as can be seen from the parameters listed in Table 1. By excluding the least luminous dSph data point, one obtains the same result (Table 1).

It follows from Eq. (1) that

$$\begin{aligned} (M_{0.3 \text{ kpc}})^{1/\kappa} &= M_0^{1/\kappa} L \quad (\kappa \neq 0), \\ M_{0.3 \text{ kpc}} &= M_0 \quad (\kappa = 0). \end{aligned} \quad (2)$$

This central mass of the DM halo can be tied by means of high-resolution CDM simulations to the total halo virial mass before its fall into the host halo (S08, see also Sect. 3),

$$M_{\text{vir}} = (M_{0.3 \text{ kpc}})^{1/0.35} \times 10^{-11} M_\odot, \quad (3)$$

yielding $M_{\text{vir}} = 10^9 M_\odot$ for $M_{0.3 \text{ kpc}} = 10^7 M_\odot$ (the common-mass scale for $\kappa = 0$). Thus, substituting $M_{0.3 \text{ kpc}}$ into Eq. (3) using Eq. (2) with $\kappa \neq 0$ leads to

$$(M_{\text{vir}})^{0.35/\kappa} = M_0^{1/\kappa} \times 10^{-(11 \times 0.35)/\kappa} L. \quad (4)$$

This value of the halo mass near $10^9 M_\odot$ for the satellites in the S08 sample is confirmed by a new analysis, in which

Wolf et al. (2010) show that the mass can be derived from a velocity dispersion profile within the deprojected 3D half light profile with minimal assumptions about the velocity anisotropy. In this way they obtain a robust mass estimator.

The observed 5σ lower value for $0.35/\kappa \equiv \eta$ is thus $\eta = 2.06$ (with $\kappa = 0.02 + 5 \times 0.03$ from Table 1).

2.2. Model Type A: internal energy sources

Dekel & Silk (1986) and Dekel & Woo (2003) studied models according to which star formation in DM halos below a total halo mass of $M_{\text{vir}} \approx 10^{12} M_{\odot}$ is governed by the thermal properties of the inflowing gas, which is regulated primarily by supernova feedback. These models demonstrate that the mass-to-light ratio of sub-halos follows $M_{\text{vir}}/L \propto L^{-2/5}$ (Eq. (24) of Dekel & Woo 2003; see also Eq. (33) of Dekel & Silk 1986). This approximately fits the observed trend for dSph satellite galaxies (Mateo 1998).

These models thus imply that

$$(M_{\text{vir}})^{\eta_{\text{th}}} = \zeta L, \quad (5)$$

where L is the total luminosity, M_{vir} is the virial DM halo mass, $\eta_{\text{th}} = 5/3$, and ζ is a proportionality factor. In essence, this relation states that more-massive halos have a larger binding energy such that it becomes more difficult to remove matter from them than from less massive halos.

Comparing with Eq. (4) and with its resulting η value as given at the end of Sect. 2.1, it follows that the observed 5σ lower value for $\eta = 0.35/\kappa = 2.06$ is in conflict with Eq. (5) where $\eta_{\text{th}} = 5/3 = 1.67$.

2.3. Model Type B1, B2: external energy source

Busha et al. (2010) follow a different line of argument to explain the dSph satellite population by employing the DM halo distribution from the *via Lactea* simulation. Here the notion is that re-ionisation would have affected DM halos variably, because of an inhomogeneous matter distribution. A given DM halo must grow above a critical mass before re-ionisation to form stars or accrete baryons. Thus the inhomogeneous re-ionisation model (Busha et al. 2010, their Fig. 6) implies, upon extraction of the theoretical data and using the same fitting method as above, theoretical κ -values of 0.15–0.17. These disagree however, with the observational value of 0.02 with a significance of more than 4σ , i.e. the hypothesis that the observational data are consistent with the models can be discarded with a confidence of 99.99 per cent (Table 1).

Busha et al. (2010) suggest that adding scatter into the theoretical description of how DM halos are filled with luminous baryons would reduce the discrepancy, but it is difficult to see how this can be done without violating the actual scatter in the observed $M_{0.3 \text{ kpc}} - L$ relation.

2.4. Model Type C: semi-analytical modelling (SAM)

Filling the multitude of DM halos with baryons given the above combined processes was investigated by Macciò et al. (2010). They semi-analytically modelled (SAM) DM sub-halos based on N -body merger tree calculations and high-resolution recomputations. The authors state “We conclude that the number and luminosity of Milky Way satellites can be naturally accounted for within the (Λ)Cold Dark Matter paradigm, and this should no longer be considered a problem.”

Their theoretical mass-luminosity data are plotted in their Fig. 5, and a fit to the redshift $z = 0$ data for $L_V > 3 \times 10^5 L_{V,\odot}$ satellites is listed in Table 1. The theoretical SAM data set shows a steep behaviour, $\kappa = 0.42$. Given the observational data, this model is ruled out with a confidence of more than ten σ .

2.5. Model Type D: high-resolution baryonic physics simulations (Aq-D-HR)

The satellite population formed in a high-resolution N -body Λ CDM re-simulation with baryonic physics of one of the MW-type “Aquarius” halos is studied by Okamoto & Frenk (2009). The treatment of baryonic processes include time-evolving photoionisation, metallicity-dependent gas cooling and photo-heating, supernova (SN) feedback, and chemical enrichment by means of SN Ia and II and AGB stars. Re-ionisation is included and the galactic winds driven by stellar feedback are assumed to have velocities proportional to the local velocity dispersion of the dark-matter halo. In these models 100 per cent of the SNII energy is deposited as thermal energy. Galactic winds are thus produced even for the least-massive dwarf galaxies. Winds are observed in strong starbursts induced through interactions rather than in self-regulated dwarf galaxies, which may pose a problem for this ansatz (Ott et al. 2005). The details of the simulations are provided by Okamoto et al. (2010). The resultant sub-halo population with stars can, as claimed by the authors, reproduce the S08 common-mass scale.

Following the same procedure as for the above models, this claim is tested by obtaining κ from their Fig. 1 (upper panel, red asterisks) and comparing it to the observational data also plotted in their Fig. 1 (note that Okamoto & Frenk 2009 plot the masses within 600 pc rather than 300 pc as used above). From their plot of the observational data, which only includes central-600 pc masses for the eight most luminous satellites, it follows that $\kappa_{\text{obs,OF}} = -0.03 \pm 0.05$. This is nicely consistent with the full S08 sample (18 satellites) discussed above. However, for their model data one finds that $\kappa = 0.17 \pm 0.02$, i.e. the model can be discarded with a confidence of 3σ or 99.7 per cent.

2.6. Model Type E1, E2: WDM

Macciò & Fontanot (2010) present theoretical distributions of satellite galaxies around a MW-type host halo for different cosmological models, namely Λ CDM and WDM with three possible DM-particle masses of $m_{\text{WDM}} = 1, 2, \text{ and } 5 \text{ keV}$. They perform numerical structure formation simulations and apply semi-analytic modelling to associate the DM sub-halos with luminous satellites. They suggest the luminosity function and mass-luminosity data of observed satellites is reproduced by the WDM models implying a possible lower limit to the WDM particle of $m_{\text{WDM}} \approx 1 \text{ keV}$.

The model and observational mass-luminosity data are compared in their fig. 5 for $m_{\text{WDM}} = 1$ and 5 keV. The slopes of these model data are listed in Table 1. From Table 1 it follows that the WDM model with $m_{\text{WDM}} \approx 1 \text{ keV}$ is ruled out with very high confidence (4σ or 99.99 per cent), and also has too few satellites fainter than $M_V \approx -8$ (their Fig. 4). WDM models with $m_{\text{WDM}} \approx 5 \text{ keV}$ are excluded at least with a 3σ or 99.7 per cent confidence, and, as is evident from their Fig. 4, the models contain significantly too few satellites brighter than $M_V = -11$.

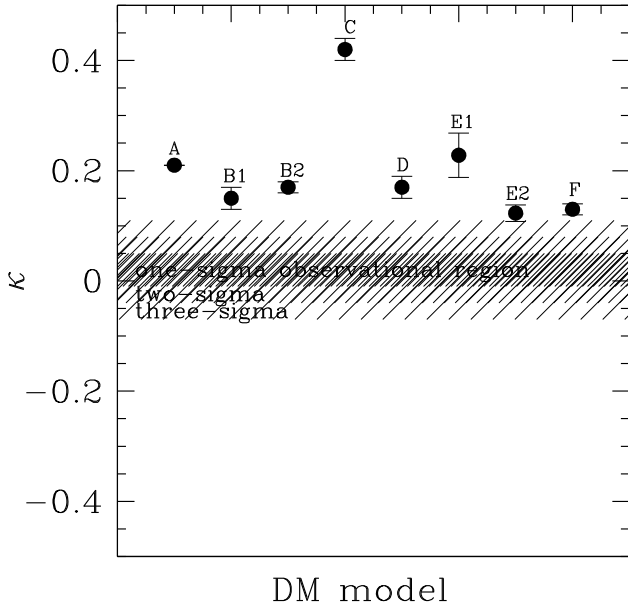


Fig. 1. The slope of the mass-luminosity relation, κ (Eq. (1)), for the models listed in Table 1. The observational constraints with confidence intervals are depicted as hatched regions (1, 2, and 3σ region). Satellites with a larger dark-matter mass are on average more luminous such that the mass-luminosity relation has $\kappa > 0$. However, the observational constraints lie in the region $\kappa \approx 0$ (see Table 1). The hypothesis that the data are consistent with any one of the models can be discarded with very high (at least 3σ , or more than 99.7 per cent) confidence.

2.7. Model Type F: infalling and disrupting dark-matter satellite galaxies

Cooper et al. (2010) study CDM model satellites in individual numerical models of dark matter halos computed within the Aquarius project. Semi-analytical modelling is employed to fill the sub-halos with visible matter, and the orbits of the infalling satellites are followed. General agreement with the observed satellites is claimed.

Much as the other models above, in this numerical CDM model of substructure and satellite formation in a MW type host halo, the MW sub-halos fall-in stochastically and therefore do not agree with the observed phase-space correlated satellites, i.e. with the existence of a rotating DoS (Sect. 5 below). Furthermore, the presented model mass-luminosity data (their Fig. 5) lead to a too steep slope (Table 1) compared to the observations and the DM-based model is excluded with a confidence of at least 99.7 per cent. In addition, Fig. 5 of Cooper et al. (2010) shows a significant increase in the number of model satellites with a similar brightness as the faintest known satellite (Segue 1, hereinafter Seg. 1). This is in contradiction with the failure to find any additional satellites of this luminosity in the most recent data mining of the existing northern SDSS data, as discussed in Sect. 6.2 below. Indeed, observations suggest that Seg. 1 is a star cluster rather than a satellite galaxy (Niederste-Ostholt et al. 2009), worsening this problem.

2.8. Discussion

In Fig. 1, the latest theoretical ansatzes A–F to solve the cosmological substructure problem are compared with the latest observational limit on the slope κ of the DM-mass-luminosity relation of dSph satellite galaxies (Eq. (1)).

The theoretical results always lead to a trend of luminosity with halo mass as a result of energy conservation. But the observed satellites do not show an increasing trend of luminosity with DM mass, according to Mateo (1998), Peñarrubia et al. (2008), and Strigari et al. (2008). From Fig. 1 we note that seven Λ CDM models of the satellites deviate 4σ or more from the data, while only one (the WDM model E2 with $m_{\text{WDM}} = 5$ keV, Table 1) deviates more than 3σ from the data. The likelihood⁵ that any of the DM models describes the data is thus less than 0.3 per cent.

As a caveat, the observed absence of a DM-mass-luminosity relation partially depends on the data for the ultra-faint dwarfs: indeed, for the classical (most luminous) dSphs, Serra et al. (2009) argue that there may be a trend, $\kappa > 0$, essentially because of their proposed increase in the mass of the Fornax dSph satellite. It is on the other hand plausible that the ultra-faint dwarfs do not possess any dark halo (see Sect. 6), and that the enclosed mass derived is due to observational artifacts. In that case they should not be used as a possible improvement for the missing satellite problem. This, however, would pose a problem for the DM hypothesis.

Adén et al. (2009b) suggest that for the Hercules dSph satellite inter-loper stars need to be removed from the observational sample, which would require a revision of the mass within 300 pc to the value $M_{0.3 \text{ kpc}} = 1.9^{+1.1}_{-1.6} \times 10^6 M_{\odot}$ (instead of the value $M_{0.3 \text{ kpc}} = 7.2^{+0.51}_{-0.21} \times 10^6 M_{\odot}$ derived by S08). This new mass measurement, however, now lies more than 4σ away from all Λ CDM-models considered above (Table 1). Hercules can thus not be understood in terms of a DM-dominated model. Adén et al. (2009b) do state that DM-free models cannot be excluded (note also Fig. 6 below), or that Hercules may be experiencing tidal disturbances in its outer parts. Tidal disturbance, however, would have to be very significant for its inner structure to be affected, because if one would require conformity with the theoretical DM-models its $M_{0.3 \text{ kpc}}$ mass would have to have been much higher and similar to the value derived by S08 ($\approx 10^7 M_{\odot}$). Given the current Galactocentric distance of Hercules of 130 kpc and the result that the inner region of a satellite is only affected by tides after significant tidal destruction of its outer parts (Kazantzidis et al. 2004), this scenario is physically implausible. There are therefore three possibilities: (i) Hercules is a DM-dominated satellite. This, however, then implies that no logically consistent solution within the CDM framework is possible because its mass-luminosity datum would lie well away from the theoretical expectation; (ii) Hercules has no DM. This implies that it cannot be used in the mass-luminosity data analysis above and would also imply there to exist an additional type of DM-free satellites, which, however, share virtually all observable physical characteristics with the putatively DM filled satellites; (iii) Hercules has been significantly affected by tides. This case is physically implausible because of its large distance, but it would imply that Hercules cannot be used in the mass-luminosity analysis above (just as Sagittarius is excluded because of the significant tidal effects it is experiencing). Omitting Hercules from the data leads to a revised observational slope $\kappa = 0.01 \pm 0.03$ such that none of the conclusions reached above about the performance of the DM-models are affected.

A point of contention for DM models of dSph satellite galaxies is that the DM halos grow at various rates and are also

⁵ The *likelihood* = $1 - (\text{confidence in per cent})/100$ gives an indication of how well the data can be accounted for by a given model. The *confidence*, as used throughout this text, is the probability level at which a model can be discarded.

truncated variously due to tidal influence. The highly complex interplay between dark-matter accretion and orbit-induced accretion truncation leads to the power-law mass function of DM halos, and at the same time would imply that the outcome in which all luminous DM sub-halos end up having the same DM mass were incompatible with the DM-theoretical expectations (see Sect. 3).

Summarising Sect. 2, while the theoretical results always lead to a trend of luminosity with halo mass, the observed satellites do not show this trend. The hypothesis that the CCM accounts for the data can be discarded with more than 99.7 per cent significance.

3. The mass function of CDM halo masses (problem 2)

One of the predictions of the Λ CDM hypothesis is the self-similarity of DM-halos down to (at least) the mass range of dwarf galaxies, i.e. that massive halos contain sub-halos of lower mass, with the same structure in a statistical sense (Moore et al. 1999a; for a major review see Del Popolo & Yesilyurt 2007). The mass function of these sub-halos is, up to a critical mass M_{crit} , well approximated by

$$\xi_{\text{sub}}(M_{\text{vir}}) = \frac{dN}{dM_{\text{vir}}} \propto M_{\text{vir}}^{-1.9}, \quad (6)$$

where dN is the number of sub-halos in the mass interval $M_{\text{vir}}, M_{\text{vir}} + dM_{\text{vir}}$ (Gao et al. 2004), M_{crit} is given by $M_{\text{vir}} \approx 0.01 M_{\text{h}}$ with M_{h} the virial mass of the hosting CDM-halo. The virial mass, M_{vir} , is defined by

$$M_{\text{vir}} = \frac{4\pi}{3} \Delta_{\text{vir}} \rho_0 r_{\text{vir}}^3, \quad (7)$$

where ρ_0 is the critical density of the Universe and Δ_{vir} is a factor such that $\Delta_{\text{vir}} \rho_0$ is the critical density at which matter collapses into a virialised halo, despite the overall expansion of the Universe. The virial radius r_{vir} is thereby determined by the density profile of the collapsed CDM-halo. For $M_{\text{vir}} > 0.01 M_{\text{h}}$, the mass function steepens (Gao et al. 2004), so that it is effectively cut off at a mass M_{max} (see Eq. (8) below). It is reasonable to identify M_{max} with the mass of the most massive sub-halo, which must be higher than M_{crit} , where the mass function begins to deviate from Eq. (6) and lower than M_{h} , the mass of the host-halo. Therefore, $M_{\text{crit}} < M_{\text{max}} < M_{\text{h}}$.

Thus, a halo with $M_{\text{vir}} \approx 10^{12} M_{\odot}$, like the one that is thought to be the host of the MW, should have a population of sub-halos spanning several orders of magnitude in mass. It is well known that, in consequence, a steep sub-halo mass function such as Eq. (6) predicts many more low-mass sub-halos than the number of observed faint MW satellites (Moore et al. 1999a; Klypin et al. 1999), a finding commonly referred to as the *missing satellite problem*. Efforts to solve this problem rely on physical processes that can either clear CDM-halos of all baryons or inhibit their gathering in the first place, which would affect low-mass halos preferentially (e.g. Moore et al. 2006; Li et al. 2010; Sect. 2). More specifically, Li et al. (2010) find that the mass function of luminous halos, $\xi_{\text{lum}}(M_{\text{vir}})$, would essentially be flat for $10^7 M_{\odot} \leq M_{\text{vir}} < 10^9 M_{\odot}$. All sub-halos with $M_{\text{vir}} \geq 10^9 M_{\odot}$ would keep baryons and therefore $\xi_{\text{lum}}(M_{\text{vir}}) = \xi_{\text{sub}}(M_{\text{vir}})$ in this mass range. Thus, the mass function of *luminous sub-halos* can be written as

$$\xi_{\text{lum}}(M_{\text{vir}}) = k k_i M_{\text{vir}}^{-\alpha_i}, \quad (8)$$

with

$$\alpha_1 = 0, \quad k_1 = 1, \quad 10^7 \leq \frac{M_{\text{vir}}}{M_{\odot}} < 10^9, \\ \alpha_2 = 1.9, \quad k_2 = k_1 (10^9)^{\alpha_2 - \alpha_1}, \quad 10^9 \leq \frac{M_{\text{vir}}}{M_{\odot}} \leq M_{\text{max}},$$

where the factors k_i ensure that $\xi_{\text{vir}}(M_{\text{vir}})$ is continuous where the power changes and k is a normalisation constant chosen such that

$$\int_{10^7}^{M_{\text{max}}} \xi_{\text{vir}}(M_{\text{vir}}) dM_{\text{vir}} = 1. \quad (9)$$

From a mathematical point of view, Eq. (8) is the probability distribution of luminous sub-halos. We note that the luminous sub-halo mass function proposed in Moore et al. (2006) is similar to the one in Li et al. (2010). In the high-mass part, it has the same slope as the mass function for all sub-halos and flattens in the low-mass part (cf. Fig. 3 in Moore et al. 2006). The lower mass limit for luminous halo is however suggested to be $M_{\text{vir}} \approx 10^8 M_{\odot}$ in Moore et al. (2006). The mass function of *all sub-halos* has $\alpha_1 \approx \alpha_2 \approx 1.9$ (Gao et al. 2004).

3.1. NFW halos

It is well established that the theoretical density profiles of galaxy-sized CDM-halos are similar to a universal law, as proposed by Navarro et al. (1997). The NFW profile is given by

$$\rho_{\text{NFW}}(r) = \frac{\delta_c \rho_0}{r/r_s (1 + r/r_s)^2}, \quad (10)$$

where r is the distance from the centre of the halo and ρ_0 is the critical density of the Universe, while the characteristic radius r_s and δ_c are mass-dependent parameters.

By integrating $\rho_{\text{NFW}}(r)$ over a volume, the total mass of CDM within this volume is obtained. Thus,

$$M(r) = \int_0^r \rho(r') 4\pi r'^2 dr' \quad (11)$$

is the mass of CDM contained within a sphere of radius r around the centre of the CDM-halo, and $M(r) = M_{\text{vir}}$ for $r = r_{\text{vir}}$. Performing the integration on the right-hand side of Eq. (11) and introducing the concentration parameter $c = r_{\text{vir}}/r_s$ leads to

$$M(r) = \frac{4\pi \rho_0 \delta_c r_{\text{vir}}^3}{c^3} \left[\frac{r_{\text{vir}}}{r_{\text{vir}} + c r} + \ln \left(1 + \frac{c r}{r_{\text{vir}}} \right) - 1 \right]. \quad (12)$$

The parameter δ_c can be expressed in terms of c ,

$$\delta_c = \frac{\Delta_{\text{vir}}}{3} \frac{c^3}{\ln(1+c) - c/(1+c)}, \quad (13)$$

as can be verified by setting $r = r_{\text{vir}}$ in Eq. (12) and substituting $M(r_{\text{vir}}) = M_{\text{vir}}$ by Eq. (7).

If the halo is luminous, it is evident that $M(r)$ is smaller than the total mass included within r , M_r . However, assuming that the MW satellites are in virial equilibrium and that their dynamics is Newtonian in the weak-field limit, the mass-to-light ratios calculated for them are generally high and imply that they are DM-dominated and thus, $M(r) = M_r$ would be a good approximation. This relation is therefore adopted for the present discussion. In this approximation $M(r = 0.3 \text{ kpc}) = M_{0.3 \text{ kpc}}$.

In principle, the parameters ρ_0 (Navarro et al. 1997), c (Bullock et al. 2001), and Δ_{vir} (Mainini et al. 2003) depend on the redshift z but for the purpose of the present paper only $z = 0$

needs to be considered, as this is valid for the local Universe. Thus,

$$\rho_0 = \frac{3H_0^2}{8\pi G}, \quad (14)$$

where the Hubble constant $H_0 = 71 \text{ km s}^{-1} \text{ Mpc}^{-1}$ (Spergel et al. 2007), $\Delta_{\text{vir}} \approx 98$ for ΛCDM -cosmology (Mainini et al. 2003), and

$$\log_{10}(\bar{c}) = 2.31 - 0.109 \log_{10}\left(\frac{M_{\text{vir}}}{M_{\odot}}\right), \quad (15)$$

where \bar{c} is the expectation value of c as a function of M_{vir} . Thus, \bar{c} decreases slowly with M_{vir} , while the scatter in the actual c is rather large, being

$$\sigma_{\log_{10} c} = 0.174 \quad (16)$$

(Macciò et al. 2007). The only caveat here is that the NFW profile is used to integrate the mass, while the now-preferred Einasto profile (Navarro et al. 2010, Sect. 1) makes only a small difference in the central parts.

3.2. Probing the ΛCDM hypothesis with $M_{0.3 \text{ kpc}}$

S08 use the stellar motions in 18 MW satellites to calculate their mass within the central 300 pc, $M_{0.3 \text{ kpc}}$. They assume the satellites to be in virial equilibrium and that Newtonian dynamics can be applied to them. The sample from S08 can be enlarged to 20 satellites by including the Large Magellanic Cloud (LMC) and the Small Magellanic Cloud (SMC), since van der Marel et al. (2002) estimated the mass of the LMC within the innermost 8.9 kpc, M_{LMC} , using the same assumptions as S08. This implies that $M_{\text{LMC}} = (8.7 \pm 4.3) \times 10^9 M_{\odot}$, of which the major part would have to be DM. Equations (7), (12), (13) and (15) have been used to create tabulated expectation values of $M(r)$ for NFW-halos with different M_{vir} and it can thereby be seen that for a typical NFW-halo with $M(r = 8.9 \text{ kpc}) = 8.7 \times 10^9 M_{\odot}$, $M(r = 0.3 \text{ kpc}) = 2.13 \times 10^7 M_{\odot} = M_{0.3 \text{ kpc}}$, and $M_{\text{vir}} = 1.2 \times 10^{11} M_{\odot}$. We note that the SMC has about 1/10th of the mass of the LMC (Kallivayalil et al. 2006), hence the virial mass of its halo can be estimated as $M_{\text{vir}} = 1.2 \times 10^{10} M_{\odot}$, corresponding to $M_{0.3 \text{ kpc}} = 1.51 \times 10^7 M_{\odot}$.

To test the shape of the MW satellite distribution function against the shape of the distribution of the $M_{0.3 \text{ kpc}}$ values of the MW-satellites, artificial samples of 10^6 $M_{0.3 \text{ kpc}}$ masses are generated in concordance with the ΛCDM hypothesis, using Monte Carlo simulations. As noted in Sect. 3.1, $M_{0.3 \text{ kpc}}$ is well approximated by $M(r = 0.3 \text{ kpc})$ in a CDM-dominated galaxy. $M(r = 0.3 \text{ kpc})$ can be calculated if M_{vir} and c are given, and the expectation value for c is a function of M_{vir} . The first step is therefore to choose a value for M_{vir} using uniform random deviates and the probability distribution of luminous halos given in Eq. (8) (see e.g. Chap. 7.2 in Press et al. 1992 for details). The next step is to attribute a value for $\log_{10}(c)$ to the chosen M_{vir} . This is done by multiplying Eq. (16) with a Gaussian random deviate and adding the result to the value for $\log_{10}(\bar{c})$, which is calculated from Eq. (15). After transforming $\log_{10}(c)$ to c , $M_{0.3 \text{ kpc}} = M(r = 0.3 \text{ kpc})$ of the given halo can be calculated from Eq. (12), using Eqs. (7) and (13). These steps are repeated, until a sample of 10^6 $M_{0.3 \text{ kpc}}$ values is generated.

If two samples are given, the maximum distance between their cumulative distribution functions, D , can be calculated. Performing the KS-test, this quantity D allows an estimate of

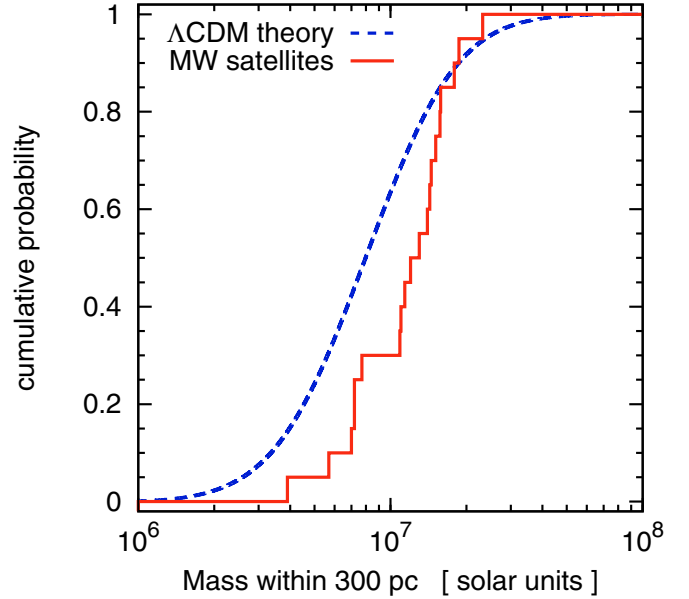


Fig. 2. The mass function of luminous satellite problem. The cumulative distribution function for the mass within the central 300 pc, $M_{0.3 \text{ kpc}}$, of the MW satellites (solid line) and the cumulative distribution function for $M_{0.3 \text{ kpc}}$ of a sample of 10^6 CDM-halos picked from the parent distribution of luminous sub-halos (Eq. (8), dashed line). The null hypothesis is that the MW satellite $M_{0.3 \text{ kpc}}$ masses are drawn from this parent distribution. The maximum distance between the two curves is 0.333 so that the null hypothesis can be discarded with 98.9 per cent confidence.

how likely it is that they are drawn from the same distribution function. The null hypothesis is that the observed satellite galaxies are drawn from the theoretically calculated mass function of luminous halos; the parent distribution is thus assumed to be the mass function of $M(0.3 \text{ kpc})$ values of luminous sub-halos according to the ΛCDM hypothesis. Assuming in Eq. (8) that $M_{\text{max}} = 10^{11} M_{\odot}$, which is approximately the mass estimated for the CDM halo of the LMC, and taking $M_{\text{min}} = 10^7 M_{\odot}$, leads to $D = 0.333$. According to the KS-test, given the parent distribution the probability of an even larger distance is 0.011. This means that the null hypothesis can be excluded with 98.9 per cent confidence. Both cumulative distributions are shown in Fig. 2⁶.

Omitting the LMC and SMC from the observational sample but keeping $M_{\text{min}} = 10^7 M_{\odot}$ and $M_{\text{max}} = 10^{11} M_{\odot}$ in the theoretical sample yields $D = 0.294$, leading to the exclusion of the null hypothesis with a confidence of 95.5 per cent. In addition setting $M_{\text{max}} = 4 \times 10^{10} M_{\odot}$, which is the M_{vir} that corresponds to the most massive $M_{0.3 \text{ kpc}}$ in the S08 sample (i.e. the most massive remaining sub-halo), yields $D = 0.301$ leading to exclusion of the null hypothesis with a confidence of 96.3 per cent. The latter two tests comprise a homogeneous mass-sample of observed satellites as compiled by S08.

That the mass function is expected to steepen at $M_{\text{crit}} = 0.01 M_h$ even increases the discrepancy between the ΛCDM

⁶ Monte Carlo experiments are used to quantify the confidence values for the KS-tests: drawing the corresponding number of sub-halo masses (e.g. 20 as in this case) from Eq. (8), D' is calculated. This is repeated 10^5 times. Counting of D' values gives the fraction of cases when $D' > D$, where D is the actually obtained D' value from the data (e.g. $D = 0.333$ in this case). These fractions are reported here as likelihood values, and are about half as large as the probability values obtained using approximate methods, as, e.g., by Press et al. (1992).

hypothesis and the observations. Reinstating the LMC and SMC back into the observational sample and cutting off $\xi_{\text{sub}}(M_{\text{vir}})$ at $M_{\text{max}} = 10^{10} M_{\odot}$ (with $M_{\text{min}} = 10^7 M_{\odot}$), which would be close to M_{crit} for the CDM-halo of the MW (see Sect. 3), and one order of magnitude below the estimated mass of the CDM-halo of the LMC, implies that $D = 0.359$ and an exclusion with 99.5 per cent confidence.

On the other hand, setting $M_{\text{max}} = 10^{12} M_{\odot}$ (with $M_{\text{min}} = 10^7 M_{\odot}$) leads to $D = 0.329$ and an exclusion with 98.8 per cent confidence. Any reasonable uncertainty in the actual value of M_{max} can therefore be excluded as an explanation of the discrepancy between the observed sample of $M_{0.3 \text{ kpc}}$ and a sample generated based on the Λ CDM hypothesis. As a consequence, the same is true for the uncertainty in the actual mass of the halo of the MW, M_{h} , since M_{max} is linked to M_{h} (see Sect. 3).

Thus M_{max} is kept at $10^{11} M_{\odot}$ in the following. Adjusting the lower limit of $\xi_{\text{lum}}(M_{\text{vir}})$ from $10^7 M_{\odot}$ to $10^8 M_{\odot}$ then leads to $D = 0.319$ and an exclusion of the null-hypothesis with a confidence of 98.4 per cent. The mass of $10^8 M_{\odot}$ is the M_{vir} suggested by the lowest $M_{0.3 \text{ kpc}}$ in the sample from S08. We note that the likelihood decreases with decreasing M_{max} , because of the overabundance of $M_{0.3 \text{ kpc}} \approx 10^7 M_{\odot}$ halos becoming more prominent in the observational sample.

S08 suggest that $\xi_{\text{lum}}(M_{\text{vir}})$ might even be cut off below a mass of $\approx 10^9 M_{\odot}$, either because halos below that mass do not contain baryons or do not form at all. Indeed, modifying $\xi_{\text{lum}}(M_{\text{vir}})$ given by Eq. (8) accordingly, results in an agreement between the theoretical distribution and the data ($D = 0.188$ with an exclusion confidence of only 70 per cent). A $\xi_{\text{lum}}(M_{\text{vir}})$ with a lower mass limit of $10^9 M_{\odot}$ is however in disagreement with the Λ CDM hypothesis, since the limiting mass below which all CDM-halos are dark ought to be two orders of magnitude lower according to Li et al. (2010).

As a final note, the newly derived reduced mass of Hercules (see end of Sect. 2.8) affects neither the calculated likelihoods nor the conclusions reached here.

Summarising Sect. 3, the mass distribution of the predicted DM halos of observed satellites is consistent with the Λ CDM hypothesis with at most 4.5 per cent likelihood. Assuming the dSph satellites are in virial equilibrium, the observationally deduced DM halo masses of the MW satellites show a significant overabundance of $M_{0.3 \text{ kpc}} \approx 10^7 M_{\odot}$ halos and a lack of less-massive values compared to the theoretically calculated distribution for luminous sub-halos, despite much effort to solve the *common-mass-scale problem* (Sect. 2).

4. The bulge mass versus satellite number relation (problem 3)

According to a straight forward interpretation of the CCM, more massive DM host halos have a larger number of luminous satellites because the number of sub-halos above a low-mass threshold increases with host halo mass, given the host halo mass waxes by accreting sub-halos. The sub-halos are accreted mostly individually without a physical link to the processes occurring at the centre of the host halo. There indeed does not appear to be an observed relation between the halo mass and the bulge mass, since pairs of galaxies with and without a bulge (such as M 31, Rubin & Ford 1970; and M101, Bosma et al. 1981, respectively) but with the same rotation velocity can be found. It would be useful to return to models A–F (Sect. 2) and to include the formation of the host galaxy in the modelling to quantify the degree of correlation between the bulge mass and number of luminous satellites actually expected in the CCM. When doing so,

the same type of models will also have to account for the presence of bulge-less galaxies having the same DM-halo mass, as pointed out above. That is, it would *not* suffice to merely demonstrate that some sort of bulge-mass-satellite number correlation emerges in the CCM. The case $M_{\text{bulge}} = 0$ must emerge naturally within the model, since two-thirds of all bright disk galaxies have no bulge or only a small one (Combes 2009b).

On the basis of extragalactic observational data, Karachentsev et al. (2005) note, but do not quantify, the existence of a correlation between the bulge luminosity and the number of associated satellite galaxies such that galaxies without a bulge have no known dSph companions, such as M 101. Karachentsev et al. (2005) also point out that the number of known dSph satellites increases with the tidal environment.

The existence of this correlation can be tested in the Local Group, where good estimates of the number of satellites within the nominal virial radii of the respective hosts and of the stellar bulge masses of the three major galaxies (MW, M 31, and M 33) exist. Only the satellites brighter than $L_V = 0.2 \times 10^6 L_{\odot}$ ($M_V < -8.44$) are considered, given that the census of fainter satellites is incomplete for the MW (notably in the southern hemisphere), and also for M 31 and M 33 given their distances. By restricting this analysis to satellites with $L_V > 0.2 \times 10^6 L_{\odot}$, the result becomes robust against the discovery of additional satellites since these would typically be fainter. The result is displayed in Fig. 3: a linear correlation between the bulge mass and the number of early-type satellites is suggested. An error-weighted least squares linear fit to the data yields

$$N_{\text{dSph}} = (4.03 \pm 0.04) \times M_{\text{bulge}} / (10^{10} M_{\odot}). \quad (17)$$

In terms of the present-day stellar mass fraction, the dSph satellites of the MW add-up to at most a few times $10^7 M_{\odot}$, so that they amount to about 0.15 per cent of the mass of the bulge. Given that Eq. (17) is a linear fit to three data points only, it will be important to check the reality of this correlation by surveying disc galaxies in the Local Volume with different bulge masses for a deep and exhaustive sampling of satellite galaxies.

Given the small number of observational data points underlying Eq. (17), one should not over-interpret this result, but it is legitimate to inquire how significant the empirical correlation between bulge mass and the number of satellites is. In view of the observation by Karachentsev et al. (2005) noted above, it may be indicative of a physical correlation.

The significance of the Local Group bulge-satellite correlation is evaluated by performing a Monte Carlo experiment, the null hypothesis of which is that there is no correlation. This hypothesis would appear to be plausible in the CCM because the number of satellites depends mostly on the host DM halo mass, while the bulge is produced by baryonic processes taking place near the center of the host DM halo. Three pairs of M_{bulge} and N_{dSph} values are chosen randomly from uniform distributions such that $M_{\text{bulge}} \in [0, 4.6 \times 10^{10} M_{\odot}]$ and $N_{\text{dSph}} \in [0, 28]^7$. For each three-point data set, a linear regression yields a measure of the degree of correlation. This is performed 10^6 times. The following incidences are counted: 1) the resulting linear relation passes the $(M_{\text{bulge}}, N_{\text{dSph}}) = (0, 0)$ point⁸ and the slope of

⁷ The upper bounds of the intervals are the 3σ upper values of M_{bulge} and N_{dSph} of M 31. The scaling of the axes is, however, irrelevant for the results of the Monte Carlo experiments, because the aim is to test how likely a correlation results, given the null hypothesis.

⁸ The precise condition here is as follows: Let there be three Monte Carlo pairs $(M_{\text{bulge}}, N_{\text{dSph}})_i$, $i = 1..3$. A linear regression yields a slope and an axis intersection, both with uncertainties expressed as σ values.

the linear relation has a relative uncertainty smaller than a given value; and the second test is 2) the slope of the linear relation has a relative uncertainty smaller than a given value. The relative uncertainty in the slope used here is based on the uncertainties in the data. Applying this relative uncertainty to Eq. (17) leads to $N_{\text{dSph}} \approx (4 \pm 1) \times M_{\text{bulge}} / (10^{10} M_{\odot})$. Taking the upper and the lower 1σ limit of the slope, this equation thereby passes the lower and the upper 1σ values of the data (Fig. 3)⁹.

The Monte Carlo result is that case 1) occurs 44 000 times, while case 2) occurs 157 000 times. Thus, if the correlation evident in Fig. 3 were unphysical, then observing it would have a likelihood of 0.044 and 0.157, respectively. Given the data on the Local Group, the above hypothesis that the bulge mass and number of satellites are not correlated can therefore be discarded with a confidence of 95.6 per cent and 84.3 per cent in case 1) and case 2), respectively.

Summarising Sect. 4, the null hypothesis that the bulge mass and the number of satellites are independent quantities is rejected, based on the Local Group data, with a confidence of more than 95.6 per cent. With the absence of a DM-mass-luminosity relation for the observed satellites (Sect. 2), this suggests that our present understanding of how satellite dwarf galaxies form and evolve may need revision. In the formation modelling of satellite galaxies within the CCM it will therefore be necessary to include also the formation of the host galaxy, to quantify the correlation between bulge mass and the number of satellites within the CCM. It will also be essential to refine this correlation using deep observational extra galactic surveys.

5. The disc of satellites (DoS) and invariant baryonic galaxies (problems 4 and 5)

The DoS is now addressed in view of the new satellite galaxies, and in Sect. 5.5 the issue that the two major DM halos of the Local Group, which happen to be similar, are occupied by similar disk galaxies is addressed within the context of the CCM.

An important constraint for understanding the origin and nature of the observed satellite galaxies comes from them being significantly anisotropically distributed about the MW, and possibly also about Andromeda. The problem of the MW system for the CCM was emphasised by Kroupa et al. (2005). They pointed out that the observed satellite system of the MW was incompatible at the 99.5 per cent confidence level with the theoretical distribution expected if the satellites were DM sub-halos tracing an isotropic DM host halo. Until then, the prediction within the DM hypothesis was that the distribution of sub-halos ought to be nearly spherical and tracing the shape of the host DM halo. For example, Aubert et al. (2004) show a MW-type DM halo to have an infall asymmetry of only about 15 per cent. The sub-halos enter the host halo along filaments and then phase-mix and virialise within the growing host DM halo. Similar sub-halo distributions are obtained in CDM and WDM models (Knebe et al. 2008).

The DoS is a pronounced feature of the MW satellite system (Metz et al. 2009b), and a similar structure was reported for the

If the axis intersection lies within 5σ of the (0, 0) point, then this particular set of bulge-satellite pairs is counted. Note that the test does not require the slope to be the same as the observed value.

⁹ The uncertainty in the slope given by Eq. (17) is a measure for how close the data lie to the straight line fitted to them, i.e. very close in the given case. However, the uncertainties on the data suggests that the observed case is rather improbable (although obviously not impossible), even if the correlation between N_{dSph} and M_{bulge} is real. The uncertainty on the slope stated in Eq. (17) would therefore not be a good basis for the test performed here.

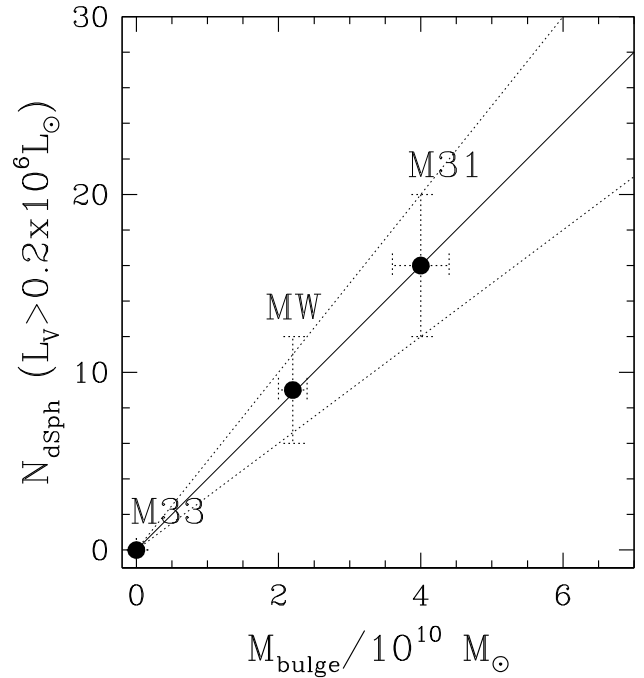


Fig. 3. The number of dSph and dE satellite galaxies more luminous than $0.2 \times 10^6 L_{\odot}$ is plotted versus the bulge mass of the host galaxy (MW: Zhao 1996, M31: Kent 1989, M33: Gebhardt et al. 2001). Only satellites within a distance of 270 kpc of the MW and M31 are used. The solid line (slope = 4.03) is Eq. (17). The upper (slope = 5.03) and the lower (slope = 3.03) dotted lines illustrate the relative uncertainty assumed in the Monte Carlo experiment (see Sect. 4).

Andromeda system (Koch & Grebel 2006) for which, however, the distance uncertainties are larger and the satellite population is richer and more complex including dSph, dE, and dIrr galaxies. In the case of the well-studied MW, the DoS is very pronounced for the classical (11 brightest) satellites including the LMC and SMC. But how are the new satellites, the ultra-faint ones, distributed? Much hope for the CCM rests on the new discoveries being able perhaps to alleviate the DoS problem.

Watkins et al. (2009) and Belokurov et al. (2010) reported the discovery of two new MW satellite galaxies, Pisces I and II, respectively, enlarging the total MW satellite system to 24 satellites. Pisces I and II were found in the southern part of the SDSS survey area, making them the two first non-classical satellite galaxies found in the southern Galactic hemisphere. Furthermore, distances to a number of the already known satellite galaxies have been updated in recent years, most notably the new distance estimate for Boo II by Walsh et al. (2008), which changes the distance from 60 to 42 kpc. An updated list of all currently known satellites is provided in Table 2 upon which the following analysis is based.

Metz et al. (2007) and Metz et al. (2009a) employed a sophisticated fitting routine to find the DoS. Here, an intuitive plane-fitting algorithm and a new disc-test are introduced. The plane-fitting algorithm leads to perfect agreement with the results obtained by Metz et al., and the new test allows an assessment of how discy the satellite distribution is.

Table 2. Data for the currently known MW satellites.

Name	α_{2000} [h m s]	δ_{2000} [° m s]	r_{helio} [kpc]	l_{MW} [°]	b_{MW} [°]	r_{MW} [kpc]	Ref.	v_{GSR}^{220} [km s ⁻¹]	v_{GSR}^{250} [km s ⁻¹]	Δv [km s ⁻¹]	Ref.	L_v [L_{\odot}]	Ref.
New:													
Boo	14 00 05	+14 30 21	64 ± 2	357.9	76.5	61	2, 10; 28; 8	94.4	94.2	±3.4	21	(2.6 ± 0.5) × 10 ⁴	2; 18
Boo II	13 58 05	+12 51 36	45 ± 2	348.6	78.9	43	30; 31; 14	64.8	69.7	±0.6	29	(9.2 ± 5.4) × 10 ²	30; 18; 31
Cygn	13 28 04	+33 33 27	214 ± 9	84.2	80.0	213	36; 8; 16; 17	64.8	69.7	±0.6	29	(2.0 ± 0.3) × 10 ⁵	36; 18
Cygn II	12 57 10	+34 19 20	154 ± 5	129.4	81.3	155	25; 3; 12; 8	-97.5	-93.2	±1.2	29	(7.5 ± 3.1) × 10 ³	25; 3; 18
CBe	12 26 59	+23 54 37	43 ± 2	202.2	75.5	44	3; 8; 23	47.4	40.4	±0.9	29	(3.1 ± 1.1) × 10 ³	3; 18; 22
Her	16 31 04	+12 47 24	135 ± 4	31.2	38.2	129	3; 7; 8; 1; 26	128.6	140.0	±1.1	29; 1	(2.9 ± 0.7) × 10 ⁴	3; 18; 26
Leo IV	11 32 58	-00 32 09	156 ± 5	261.1	56.3	156	3; 20	10.6	-6.0	±1.4	29	(1.3 ± 0.3) × 10 ⁴	3; 18; 27; 9
Leo V	11 31 09	+02 13 05	176 ± 10	257.9	58.3	176	4; 9	58.5	42.8	±3.1	4	(6.4 ± 2.4) × 10 ³	4; 9
Pis I	23 40 00	-00 18 00	80 ± 14	100.2	-57.8	80	32; 15	42.1	58.0		15		
Pis II	22 58 31	+05 57 09	182 ± 36*	84.1	-47.6	181	6					~8.6 × 10 ³	6
Seg I	10 07 04	+16 04 40	23 ± 2	206.2	39.5	28	3	94.5	79.3	±1.3	11	(3.4 ± 2.7) × 10 ²	3; 18
Seg II	02 19 16	+20 10 31	35 ± 2	157.0	-31.1	41	5	54.8	67.6	±2.5	5	(8.6 ± 2.7) × 10 ²	5
UMA	10 34 49	+51 55 48	100 ± 4	162.0	51.3	105	34; 29; 24	-6.9	-0.3	±1.4	29	(1.4 ± 0.4) × 10 ⁴	18
UMA II	08 51 30	+63 08 22	30 ± 5	159.7	30.4	37	35	-29.0	-17.1	±1.9	29	(3.3 ± 1.0) × 10 ³	35; 18; 22
Will	10 49 22	+51 03 10	41 ± 6	164.4	48.8	46	33; 8					(1.1 ± 0.6) × 10 ³	33; 18
Classical:													
Car [†]	06 41 37	-50 58 00	101 ± 5	255.2	-21.7	103	19	22.5	-4.9	±3	19	4.5 × 10 ⁴	19
Dra [†]	17 20 19	+57 54 48	82 ± 6	93.5	34.6	82	19	-112.3	-87.7	±2	19	2.8 × 10 ⁵	19
For [†]	02 39 59	-34 27 00	138 ± 8	230.0	-63.4	140	19	-29.2	-40.4	±3	19	1.6 × 10 ⁷	19
Leo I	10 08 27	+12 18 30	250 ± 30	224.7	48.6	254	19	179.9	165.4	±2	19	4.9 × 10 ⁶	19
Leo II	11 13 29	+22 09 12	205 ± 12	217.5	66.1	208	19	17.0	9.0	±2	19	5.9 × 10 ⁵	19
LMC [†]	05 23 34	-69 45 24	49 ± 2	268.5	-33.4	48	19	143.3	118.6		19	2.1 × 10 ⁹	37
SMC [†]	00 52 44	-72 49 42	58 ± 2	291.6	-47.4	55	19	49.6	32.5		19	5.7 × 10 ⁸	37
Sgr [†]	18 55 03	-30 28 42	24 ± 2	9.4	-22.4	16	19	161.1	164.0	±5	19	2.0 × 10 ⁷	19
Scu [†]	01 00 09	-33 42 30	79 ± 4	234.6	-81.9	79	19	77.9	73.8	±3	19	2.4 × 10 ⁶	19
Sex	10 13 03	-01 36 54	86 ± 4	237.8	40.8	89	19	76.9	56.4	±3	19	5.4 × 10 ⁵	19
UMI [†]	15 09 11	+67 12 54	66 ± 3	114.2	43.2	68	19	-92.9	-71.7	±2	19	3.1 × 10 ⁵	19

Notes. Data for the MW satellites used for fitting the DoS, Seg 1 and 2 (marked in *italics*) are included in this list for reference, but they have not been included in the fitting because they appear to be diffuse star clusters (Niederste-Ostholz et al. 2009). The positions are given both in Heliocentric coordinates (right ascension α_{2000} , declination δ_{2000} , and Heliocentric distance r_{helio} for epoch J2000.0) and in Galactocentric coordinates assuming the Sun to have a distance of 8.5 kpc from the centre of the MW. l_{MW} gives the Galactic longitude using data from the references listed in the column labelled Ref., where more than one source is given, the distances to the satellites were obtained by error-weighted averaging over the available measurements. The satellite's line-of-sight velocities with respect to the Galactic standard of rest (GSR) are calculated assuming the Sun to move into the direction $l = 90^\circ$, $b = 0^\circ$ (in Heliocentric, Galactic coordinates) with a velocity of either 220 km s^{-1} (v_{GSR}^{220}) or 250 km s^{-1} (v_{GSR}^{250}). The measurement-uncertainties for the radial velocities reported in the respective papers (referred to in column Ref.) are reproduced in the column labelled Δv . Finally, L_v gives the satellite luminosities in the photometric V-band; again uncertainty-weighted averages are quoted when more than one reference is given in column Ref. Data marked with † have measured proper motions, listed in Table 1 of Metz et al. (2008). *, As no distance uncertainties for Pisces II are available in the literature, the error is estimated to be 20 percent of the distance.

References. 1: Adén et al. (2009a), 2: Belokurov et al. (2006), 3: Belokurov et al. (2007), 4: Belokurov et al. (2008), 5: Belokurov et al. (2009), 6: Belokurov et al. (2010), 7: Coleman et al. (2007b), 8: de Jong et al. (2008), 9: de Jong et al. (2010), 10: Dall'Ora et al. (2006), 11: Geha et al. (2009), 12: Greco et al. (2008), 13: Ibata et al. (2006), 14: Koch et al. (2009), 15: Kollmeier et al. (2009), 16: Kuhn et al. (2008), 17: Martin et al. (2008a), 18: Martin et al. (2008b), 19: Mateo (1998), 20: Moretti et al. (2009), 21: Muñoz et al. (2006), 22: Muñoz et al. (2010), 23: Musella et al. (2009), 24: Okamoto et al. (2008), 25: Sakamoto & Hasegawa (2006), 26: Sand et al. (2009), 27: Sand et al. (2010), 28: Siegel (2006), 29: Simon & Geha (2007), 30: Walsh et al. (2007), 31: Walsh et al. (2008), 32: Watkins et al. (2009), 33: Willman et al. (2005a), 34: Willman et al. (2005b), 35: Zucker et al. (2006a), 36: Zucker et al. (2006b), 37: van den Bergh (1999).

5.1. Parameters of the DoS

A simple and straightforward method is described to calculate the DoS parameters l_{MW} , b_{MW} , D_{p} , and Δ , which are, respectively, the direction of the DoS-normal vector in Galactic longitude and latitude, the smallest distance of the DoS plane to the Galactic centre, and the root-mean-square height (half the thickness) of the DoS.

The positions of satellites on the sky and their radial distances (compiled for convenience in Table 2) are transformed into a Galactocentric, cartesian coordinate system assuming the distance of the Sun to the centre of the MW to be 8.5 kpc. The z -coordinate points into the direction of the Galactic north pole and the Sun lies in the MW disk plane.

The 3D coordinates are projected into two dimensions, plotting z against a projection onto a plane defined by the Galactic longitude l_{MW} . This resembles a view of the MW satellite system as seen from infinity and from within the MW disc plane. The view of the satellite system is rotated in steps of 1° . For each step, a linear fit is made to the projected satellite distribution. The linear fit is determined using the least squares method, demanding the satellite-distances, as measured perpendicularly to the fitted line, to become minimal. This line constitutes a plane seen edge-on in the current projection. The two free parameters of the fit are the closest distance from the MW centre, D_{p} , and the inclination b_{MW} of the normal vector to the z -axis (a polar plane has $b_{\text{MW}} = 0^\circ$). The plane-normal-vector's longitude is l_{MW} , given by the projection. The fits are performed for each angle l_{MW} between 0° and 360° . After half of a rotation, the view is identical to the one of 180° before, mirrored along the z -axis.

For each angle l_{MW} , the root mean square (rms) height, Δ , of the satellite distribution around the fitted line is determined. The normal vector to the best-fit disc solution (the DoS) to the full 3-dimensional distribution of the MW satellites is then given by those l_{MW} and b_{MW} that give the smallest rms height Δ_{min} .

To account for the uncertainties in the distance of the satellites, the major source of error, the procedure is repeated 1000 times. Each time, the radial position of each satellite is randomly chosen from a normal distribution centered on the satellite's radial distance. It has a standard deviation given by the distance uncertainties to the satellite galaxies. Once a realisation with varied radial distances is set up, the coordinate transformation into the Galactic coordinate system is performed. The parameters of the best fits are determined for each realisation. Their final values are determined by averaging the results of all realisations, the standard deviations of their values are adopted as the uncertainties in the fits.

Fitting all 24 currently known satellite galaxies within a distance of 254 kpc from the MW, the minimum disc height is found to be $\Delta_{\text{min}} = 28.9 \pm 0.6$ kpc. This is more than 14σ away from the maximum height of $\Delta_{\text{max}} = 55.7 \pm 1.3$ kpc obtained at a 90° projection of the data. *Thus, the DoS is highly significant.* The position of the minimum height gives the best-fit disc, the DoS. The normal vector defining the DoS points to $l_{\text{MW}} = 156.4 \pm 1.8$ and has an inclination of $b_{\text{MW}} = -2.2 \pm 0.6$, i.e. is nearly perfectly polar. D_{p} , the closest distance of the DoS from the MW centre, is 8.2 ± 1.0 kpc $\ll \Delta_{\text{min}}$.

5.2. A novel disc test

Another test to determine whether the satellite galaxies are distributed in a disc can be performed by comparing the number of satellites near the plane to the number further away: let N_{in} be the number of all satellites that have a perpendicular distance of

less than 1.5 times the minimal disc height Δ_{min} from the line-fit. Accordingly, N_{out} represents all satellites further away. Both N_{in} and N_{out} are determined for each rotation angle, measuring distances from the line (i.e. plane viewed edge-on in the given projection) that fits the distribution in the given projection best. This is illustrated in Fig. 4. It shows an edge-on view of the best-fit plane, along with a view rotated by 90° . Both views see the disc of the MW edge-on.

Figure 5 shows the ratio of galaxies found within the DoS to those outside (solid black line), $\mathcal{R} = N_{\text{in}}/N_{\text{out}}$. The situation is shown for the unvaried distances. If the MW satellites were distributed in a disc, \mathcal{R} would approach a maximum when looking edge-on, while it will rapidly decrease once the projection is rotated out of the disc plane. It is a good test to discriminate a disc-like distribution from a spheroidal one. The latter would not lead to much variation in the ratio.

It can be seen that \mathcal{R} approaches a maximum close to the best-fit l_{MW} . At the maximum, only two of the 24 satellite galaxies are found outside of the required distance from the disc. The maximum \mathcal{R} is thus 11.0, situated only a few degrees away from the l_{MW} that gives the smallest height. This has to be compared to the broad minimum of $\mathcal{R} \approx 1$. The disc-signature is obvious, proving the existence of a DoS that incorporates the new satellites found in the SDSS.

5.3. Classical versus new satellites: is there a DoS in both cases?

In addition to the above analysis of all 24 known MW satellites, the analysis is also carried out separately for two distinct subsamples: the 11 classical, most-luminous satellite galaxies and the 13 new satellites discovered mostly in the SDSS. Each of them uses an own minimal height, given by the subsample distribution, in determining \mathcal{R} . If all satellite galaxies follow the same distribution, given by the DoS, a separate fitting should lead to similar parameters. If, on the other hand, the new (mostly ultra-faint) satellites follow a different distribution, then this would challenge the existence of a DoS. *It is worth emphasising that while the brightest satellites in a Λ CDM model of a MW-type halo may exceptionally form a weak disc-like structure (Libeskind et al. 2009), none of the existing CCM-based theoretical satellite distributions predict the whole luminous satellite population to be disc-like.*

Furthermore, comparing the results for the classical 11 satellites with the ones obtained by the more sophisticated fitting technique used by Metz et al. (2007) is a good test to check whether the present technique gives reliable results.

The graphs for both subsamples are included in Fig. 5, the results for classical satellites are represented by the dashed yellow, the new (SDSS) satellite galaxies by the dashed green line. Both are in good agreement not only with the combined sample, but also with each other. They peak at their best-fit l_{MW} , with each of them having an N_{out} of only one galaxy at the peak.

Applying the technique presented in Sect. 5.1 to calculate the DoS parameters, the new satellites have a best-fit disc with a normal vector pointing to $l_{\text{MW}} = 151.4 \pm 2.0$, only five degrees away from the direction that was obtained by considering all known MW satellites. The inclination is $b_{\text{MW}} = 9.1 \pm 1.0$, again an almost perpendicular orientation of the DoS relative to the MW disc, being only 11 degrees away from the value determined before. The derived rms height is $\Delta_{\text{min}} = 28.6 \pm 0.5$ kpc, essentially identical to the one given by all satellite galaxies. The minimum distance from the MW centre is $D_{\text{p}} = 18.3 \pm 1.3$ kpc.

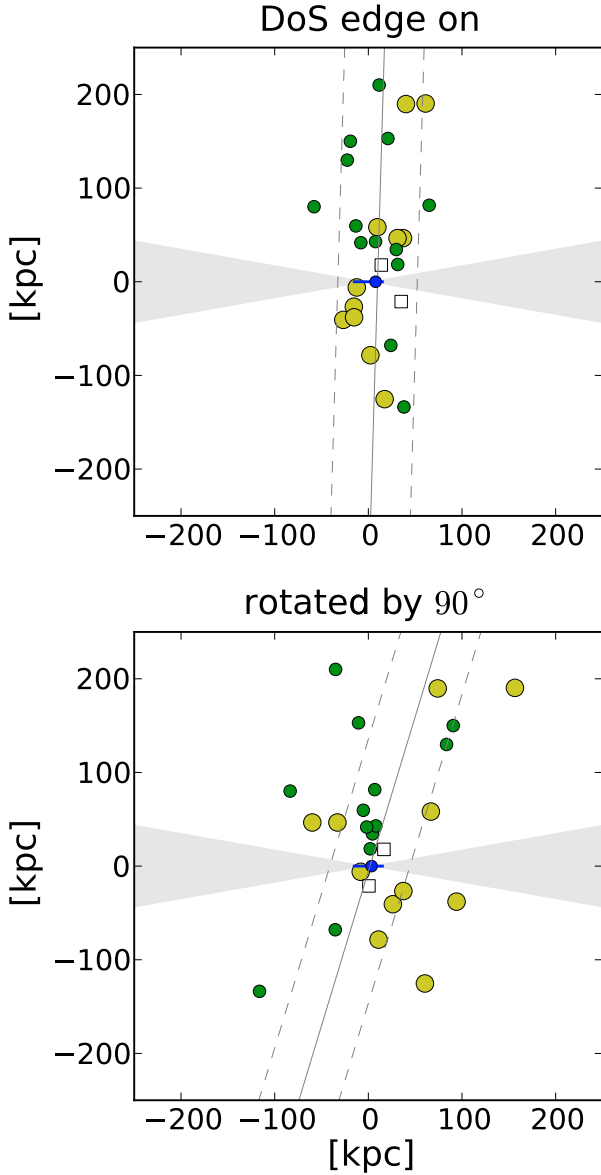


Fig. 4. Parameters of the MW DoS: the 3-D distribution of the MW satellite galaxies. The 11 classical satellites are shown as large (yellow) circles, the 13 new satellites are represented by the smaller (green) dots, whereby Pisces I and II are the two southern dots. The two open squares near the MW are Seg 1 and 2; they are not included in the fit because they appear to be diffuse star clusters nearby the MW, but they do lie well in the DoS. The obscuration-region of $\pm 10^\circ$ from the MW disc is given by the horizontal gray areas. In the centre, the MW disc orientation is shown by a short horizontal line, on which the position of the Sun is given as a blue dot. The near-vertical solid line shows the best fit (seen edge-on) to the satellite distribution at the given projection, the dashed lines define the region $\pm 1.5 \times \Delta_{\min}$, Δ_{\min} being the rms-height of the thinnest DoS ($\Delta_{\min} = 28.9$ kpc in both panels). *Upper panel:* an edge-on view of the DoS. Only three of the 24 satellites are outside of the dashed lines, giving $N_{\text{in}} = 21$, $N_{\text{out}} = 3$ and thus a ratio of $\mathcal{R} = N_{\text{in}}/N_{\text{out}} = 7.0$. Note the absence of satellites in large regions of the SDSS survey volume (upper left and right regions of the upper panel, see also Fig. 1 in Metz et al. 2009a, for the SDSS survey regions). *Lower panel:* a view rotated by 90° , the DoS is seen face-on. Now, only 13 satellites are close to the best-fit line, 11 are outside, resulting in $\mathcal{R} = 1.2$. Note that by symmetry the Southern Galactic hemisphere ought to contain about the same number of satellites as the Northern hemisphere. Thus, *The Stromlo Milky Way Satellite Survey* is expected to find about eight additional satellites in the Southern hemisphere.

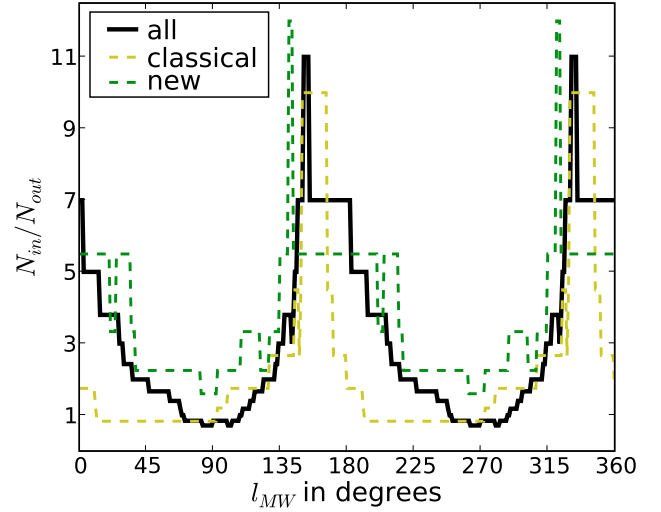


Fig. 5. Testing for the existence of the DoS. The behaviour of \mathcal{R} for each view of the MW, given by the Galactic longitude of the normal vector for each plane-fit. $\mathcal{R} = N_{\text{in}}/N_{\text{out}}$ is the ratio of the number of satellites within $1.5 \times \Delta_{\min}$ ($\Delta_{\min} = 28.9$ kpc), N_{in} , to those further away from the best-fit line, N_{out} , calculated for all 24 known satellites, as well as for the fits to the 11 classical and the 13 new satellites separately (taking their respective rms heights as the relevant Δ_{\min}). The disc-like distribution can be clearly seen as a strong peak close to $l_{\text{MW}} = 150^\circ$. Note that the position of the peaks are close to each other for both subsamples separately. This shows that the new satellite galaxies independently define the same DoS as the classical satellite galaxies.

The fitting to the 11 classical satellites leads to results that are in very good agreement, too. The best-fit position for the 11 classical satellites is $l_{\text{MW}} = 157:6 \pm 1:1$ and $b_{\text{MW}} = -12:0 \pm 0:5$, the height is found to be $\Delta = 18.3 \pm 0.6$ kpc, and the closest distance to the MW centre is $D_{\text{P}} = 8.4 \pm 0.6$ kpc. This is in excellent agreement with the results of Metz et al. (2007). In that paper, the authors reported that $l_{\text{MW}} = 157:3$, $b_{\text{MW}} = -12:7$, $\Delta_{\min} = 18.5$ kpc, and $D_{\text{P}} = 8.3$ kpc. This illustrates that the results are extremely accurate despite employing a more simple disc-finding technique.

The agreement of the fit parameters for the two subsamples *separately* is impressive. Two populations of MW satellite galaxies (classical versus ultra-faint) with different discovery histories and methods define the same DoS. This shows that the new, faint satellites fall close to the known, classical, DoS ($\equiv \text{DoS}_{\text{cl}}$). Even without considering the classical satellite galaxies, the new satellites define a disc, DoS_{new} , that has essentially the same parameters. This confirms the existence of a common $\text{DoS} \approx \text{DoS}_{\text{new}} \approx \text{DoS}_{\text{cl}}$.

5.4. The DoS – discussion

A pronounced DoS is therefore a physical feature of the MW system. But what is its origin? Is the existence of both the classical-satellite DoS_{cl} and the new-satellite DoS_{new} , such that $\text{DoS}_{\text{new}} \approx \text{DoS}_{\text{cl}}$, consistent with the CCM?

It has been suggested that the highly anisotropic spatial satellite distribution maps a highly prolate DM halo of the MW that would need to have its principal axis oriented nearly perpendicularly to the MW disc (Hartwick 2000). However, there is still much uncertainty and disagreement as to the shape and orientation of the MW DM halo: Fellhauer et al. (2006) used the bifurcation of the Sagittarius stream to constrain the shape of

the MW DM halo to within about 60 kpc, finding it to be close to spherical. The measurement of the shape of the DM halo of the MW within 60 kpc by Law et al. (2009), also based on the Sagittarius stream, suggests that the DM halo is triaxial, but with major and minor axes lying within the plane of the MW disc. The DM halo of the MW would therefore not trace a similar three-dimensional structure as the satellites, unless the major axis of the MW halo changes its orientation by about 90 degrees beyond 60 kpc and becomes essentially disc-like (i.e. highly oblate). Law & Majewski (2010) find a new slightly oblate solution to the MW DM halo shape at distances from 20 to 60 kpc. In this solution, the minor axis points along the line Sun-MW-centre suggesting a similar orientation of this extra potential as the DoS. The authors emphasise that this model is not strongly motivated within the current CDM paradigm, it merely serving as a “numerical crutch”. Given this disagreement about the shape and orientation of the MW DM halo, a significant future observational and theoretical effort to clarify the situation is needed.

An additional issue for the CCM is that the normal to the DoS is defined mostly by the outermost satellites, while the direction of the average orbital angular momentum vector is defined by the innermost satellites for which proper motions have been measured. Both, the normal and the average orbital angular momentum vector are nearly co-aligned implying a strong degree of *phase-space correlation* between the satellites such that the DoS is rotating (Metz et al. 2008). This rotational DoS is not expected if the satellites merely trace the MW DM halo, because they would have independent infall histories and would therefore not be correlated in phase space.

This phase-space feature has been addressed by Libeskind et al. (2009). In a thorough analysis of structure formation on MW-galaxy scales, they show that the MW constitutes an improbable but possible constellation of CDM-dominated satellites about a MW-type disk galaxy, the satellites having (of course) independent infall and accretion histories.

They analyse an N-body sample of 30946 MW-mass DM host halos with mass in the range $2 \times 10^{11} M_{\odot}$ to $2 \times 10^{12} M_{\odot}$ for the properties of their substructure distribution. They first select from this sample only those halos that host a galaxy of similar luminosity as the MW (specifically, galaxies more luminous in the V-band than $M_V = -20$). From this remaining sample of 3201 (10 per cent) hosts, they select those that contain at least 11 luminous satellites, leaving 436 (1.4 per cent) host halos. In this sample of 436 systems, about 30 per cent have 6 luminous satellites with orbital angular momenta aligned to a degree similar to that of the MW system. Thus, only 0.4 per cent of all existing MW-mass CDM halos would host a MW-type galaxy with the right satellite spatial distribution. As the authors point out, this probability of 4×10^{-3} that the DM model accounts for the observed MW-type satellite system would be lower still if proper motion measurements of additional satellites affirm the orbital angular momentum correlation highlighted by Metz et al. (2008), or if the satellites that may be discovered in the southern hemisphere by the *Stromlo Milky Way Satellite Survey* (Jerjen 2010)¹⁰ also lie within the DoS. All 13 new satellites define the same DoS as the 11 classical ones, and furthermore, the latest additions in the southern Galactic hemisphere also lie in the DoS (Sect. 5.3), suggesting that the DM hypothesis is much less likely than 0.4 per cent to be able to account for the MW satellite system in MW-type DM halos.

Li & Helmi (2008) and D’Onghia & Lake (2008) propose an interesting alternative solution to the *satellite*

phase-space correlation problem: they suggest that the correlation is caused by the infall of groups of DM-dominated dwarf galaxies. Unfortunately, this proposition is challenged by all known nearby groups of dwarf galaxies being spatially far too extended to account for the thinness of the DoS (Metz et al. 2009b). It may be thought that the groups that have fallen in correspond to compact dwarf groups that do not exist any longer because they have subsequently merged. But this is compromised by the observation that their putative merged counterparts in the field do not seem to exist (Metz et al. 2009b). Indeed, Klimentowski et al. (2010) model a MW-type system and deduce “... that such a disc is probably not an effect of a group infall unless it happened very recently” (their Sect. 4.2.2). Furthermore, this notion would seem to imply that dwarf galaxy groups are full of dSph galaxies, while the pristine (before group infall) MW halo would have formed none, in conflict with the observed morphology-density relation (e.g. Okazaki & Taniguchi 2000).

It needs to be emphasised that the DM-based models have so far not addressed the issue that the DoS lies nearly perpendicularly to the MW disc; DM-based models need to *postulate* that this occurs, and it may indeed simply be chance. The combined probability that a DM-based model accounts for the observed MW-type system, which has the properties that the satellites have correlated angular momenta and form a DoS highly inclined to the baryonic disc of the host galaxy, cannot currently be assessed but is, by logical implication, smaller than 4×10^{-3} .

But perhaps the MW is a very special system, an outlier within the DM-based framework? This possibility can be assessed by considering the nearest MW-similar DM halo. It hosts a similar disc galaxy, Andromeda, which has a similar satellite system to the MW but is however richer and more complex, and has a larger bulge mass than the MW (Fig. 3). Andromeda may also have a DoS (Koch & Grebel 2006; see also Fig. 4 in Metz et al. 2009a)¹¹ suggesting that these satellite distributions may not be uncommon among MW-type DM halos.

Thus, a Local Group consisting of two dominant DM halos of similar (MW-type) mass would have a likelihood of 0.4 per cent times 1.4 per cent, i.e. 5.6×10^{-5} , to appear with two MW-type disc galaxies, one of them having a pronounced rotating DoS with 11 or more luminous satellites, and the other having at least 11 luminous satellites.

5.5. Invariant baryonic galaxies

The Libeskind et al. (2009) analysis, described in Sect. 5.4, also shows that about 10 per cent of MW-type DM halos would host a MW-luminous galaxy, the 90 per cent of others would presumably host galaxies with lower luminosities suggesting a large variation between DM halo and luminous galaxy properties. This however, appears to be a problem considering the properties of observed disc galaxies. By using a principal component analysis on hundreds of disc galaxies, Disney et al. (2008) demonstrate that observed disc galaxies are simple systems defined by one underlying parameter, rather than about six if the galaxies were immersed in DM halos. Citing additional similar results, van den Bergh (2008) and Gavazzi (2009) reach the same conclusion, as well as Gentile et al. (2009) and Milgrom (2009a). This is further supported by an entirely independent study of star-forming galaxies, which again shows a remarkably small variation of behaviour (Pflamm-Altenburg & Kroupa 2009b). The discovery that the ratio of DM mass to baryonic mass within

¹⁰ http://www.mso.anu.edu.au/~jerjen/SMS_Survey.html

¹¹ Note that the rich satellite system of M 31 may have a sub-population of satellites in a disc-like structure (Metz et al. 2009a).

the DM core radius is constant for galaxies (Sect. 6.4.1 below) is another statement of the same effect.

The small amount of variation for disc galaxies thus appears to be very difficult to reconcile with the large variation inherent in the DM model, as quantified by the Libeskind et al. (2009) analysis: 90 per cent of MW-mass DM halos would have disc galaxies that differ substantially in luminosity from the MW in the CCM, and yet the closest neighbour, Andromeda, is similar to the MW. This is the *invariant-baryonic-galaxy problem*.

Summarising Sect. 5, the CCM is highly significantly challenged by the spatial distribution of MW satellite galaxies and by the similarity of rotationally supported galaxies. The *phase-space correlation problem* of the classical satellites is enhanced significantly after the inclusion of the new ultra-faint satellites, and the Local Group enhances the *invariant baryonic galaxy problem*.

6. The origin of dSph and dE galaxies: The Fritz Zwicky Paradox, an alternative proposition and deeper implications

What has been learned so far? The DM-mass-luminosity data of MW dSph satellite galaxies appear to be in conflict with the CCM results, and the mass function of DM masses of the dSph satellites is not in good agreement with the mass function of luminous sub-halos calculated within the CCM. The correlation bulge-mass versus satellite-number is tentative (for having only three points) but will very likely pass the test of time because the error bars allow for a conclusive significance test. The two quantities appear to be physically related as indicated strongly by the Local Group data and also extragalactic surveys, but clearly much more work needs to be done both observationally and theoretically to refine the implied correlation. The highly pronounced phase-space correlation of the MW satellites means that any formation mechanism must have involved correlated orbital angular momenta of the satellites.

Given that the formation of a bulge involves highly dissipative processes, it emerges that a highly dissipative process seems to have formed the bulge and the correlated orbital angular momenta of the satellites. This leads to the real possibility that the origin of both the MW bulge and its satellite population is related to a galaxy-galaxy encounter. Indeed, it is well known and documented that galaxy encounters lead to the formation of bulges and tidal arms that can host the formation of tidal-dwarf galaxies (TDGs). These are then naturally correlated in phase space. Since the bulge and the satellites of the MW are about 11 Gyr old, we are led to the scenario that the proto-Galaxy may have had a major encounter or merger about 11 Gyr ago during which the bulge and the satellites formed (Pawlowski et al. 2010). Wetzstein et al. (2007) demonstrated in a series of numerical models that the number of TDGs increases indeed with the gas fraction of the pre-collision galaxy. This is relevant to galaxy encounters at a high redshift, where galaxy encounters are expected to have been frequent.

Noteworthy is that a scenario for the origin of dSph satellite galaxies along the above lines had been suggested already before the DM hypothesis was widely accepted, namely that they may be ancient TDGs (Lynden-Bell 1976; Lynden-Bell 1983; Kunkel 1979). This proposition can naturally account for their correlated phase-space distribution in the form of a rotating disc-like distribution (Sect. 5), and would lend a new viewpoint on the difficulty of understanding the properties of the MW dSph satellites

as DM sub-halos documented above. Indeed, in a famous conjecture, Zwicky (1956, on p. 369) states that new dwarf galaxies form when galaxies interact. As shown here this leads to a contradiction with observational data when this conjecture is combined with his other famous conjecture according to which the masses of galaxies are dominated by dark matter (Zwicky 1937). This contradiction is referred to as the Fritz Zwicky Paradox.

6.1. The evolution of TDGs

A natural way to explain the satellite phase-space correlation as well as the bulge-satellite relation is thus to identify the dSph satellite galaxies of the MW with a population of ancient TDGs that probably formed during a gas-rich encounter between the early MW and another galaxy. But if they all formed at the same time, how can the different chemical properties and star-formation histories of the different dwarf galaxies then be explained within this scenario? If the DM hypothesis is not viable for the MW satellite population, how can the high mass-to-light ratios of the satellites be explained?

It is known that the satellite galaxies all have ancient populations of an indistinguishable age (Grebel 2008), perhaps being created when the TDGs were born. Or, the ancient population comes from the precursor host galaxy. TDGs may also form with globular clusters as long as the star-formation rate surpasses a few M_{\odot}/yr for 10 Myr (Weidner et al. 2004). The chemo-dynamical modelling by Recchi et al. (2007) has shown that once a TDG (without DM) forms it is not natural for it to blow out the gas rapidly. Rather, the rotationally-supported small gas-rich discs of young TDGs begin to evolve through self-regulated star formation either until their gas is consumed or removed through ram-pressure stripping. Consequently, their internal evolution through star formation can be slow and individual, such that TDGs that formed during one encounter event can exhibit different chemical properties many Gyr after their formation. Removal of the interstellar medium from the TDG through ram-pressure takes about half to a few orbital times, which is typically one to a few Gyr after formation. This time scale is consistent with the observed cessation of star formation in most MW dSph satellites (Grebel 1999). The TDGs that have remained at large distances from their hosts retain their gas and appear as dIrr galaxies (Hunter et al. 2000). Once formed, TDGs cannot fall back onto their hosts and merge since dynamical friction is insignificant for them. A TDG may be dispersed (but not accreted) if it happens to be on a near radial orbit, which, however, is unlikely given the torques acting on the tidally expelled material from which the TDG forms during the encounter.

If the dSph satellites are ancient TDGs then understanding their internal kinematics remains a challenge though because TDGs do not contain significant amounts of DM (Barnes & Hernquist 1992; Wetzstein et al. 2007; Bournaud et al. 2007; Gentile et al. 2007; Milgrom 2007). However, the inferred large M/L ratios of dSph satellites (and especially of the ultra-faints) may not be physical values but may be a misinterpretation of the stellar phase-space distribution within the satellite. If this were to be the case then the absence of a “DM-mass”-luminosity relation (Sect. 2) for dSph satellites would be naturally understood.

The following gedanken-experiment illustrates that this could be the case. An unbound population of stars on similar orbits, each slightly inclined relative to the other orbits, will reconfigure at apogalacticon and an observer would see a stellar phase-space density enhancement and would also observe a velocity dispersion. The M/L ratio calculated from the observed velocity dispersion would not be a true physical

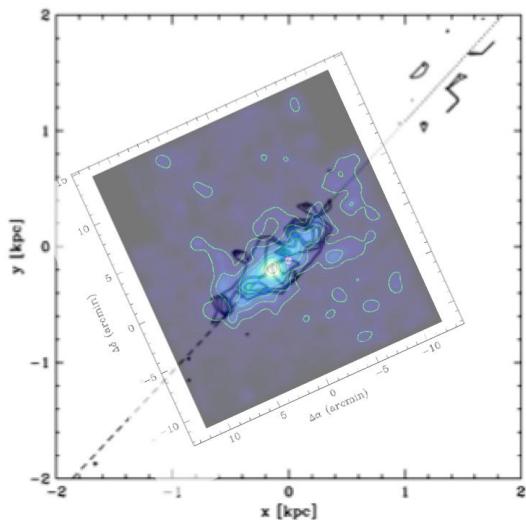


Fig. 6. Model RS1-5 from Kroupa (1997) (on the kpc grid) is plotted over the surface brightness contours of Hercules by Coleman et al. (2007a) (celestial coordinate grid). The dashed and dotted curve are, respectively, the past and future orbit of RS1-5.

M/L ratio. Models related to this idea have been studied by Kuhn (1993). Moreover, resonant orbital coupling can periodically inflate kinematically measured M/L values (Kuhn & Miller 1989; Kuhn et al. 1996). Fully self-consistent Newtonian N -body models have demonstrated that unphysically high M/L ratios arise indeed if TDGs are allowed to orbit a host galaxy sufficiently long such that the remaining stellar population within the ancient TDG adopts a highly non-isotropic phase-space distribution (Kroupa 1997; Klessen & Kroupa 1998; Metz & Kroupa 2007). These models suggest that it may be wrong to use an observed velocity dispersion to calculate a mass for a dSph satellite. Thus, tidal shaping of TDGs over a Hubble time can produce remnant objects that have internal highly-anisotropic stellar phase-space distributions that would be falsely interpreted by an observer as corresponding to a high M/L ratio, as explicitly shown by Kroupa (1997). Intriguingly, these models reproduce the gross physical parameters of dSph satellites well (Metz & Kroupa 2007), and thus constitute the simplest available stellar dynamical solutions of dSph satellites constructed without fine-tuning.

It is indeed remarkable how model RS1-5 of Kroupa (1997), shown here as a snapshot (Fig. 6), is an essentially perfect match to the dSph satellite Hercules (see Fig. 2 in Coleman et al. 2007a) discovered 10 years later by Belokurov et al. (2007). The half-light radius is 180 pc in the model and 168 pc for Hercules, RS1-5 has a velocity dispersion of about 2.8 km s^{-1} (Table 2 in Kroupa 1997), while Hercules has a measured velocity dispersion of $3.72 \pm 0.91 \text{ km s}^{-1}$ (Adén et al. 2009a), and the inferred mass-to-light ratio that one would deduce from velocity dispersion measurements based on the assumption of equilibrium is about 200 in both cases. Both RS1-5 and Hercules have luminosities agreeing within one order of magnitude (the model being the brighter one), yet RS1-5 has no DM.

The TDG models for dSph satellites proposed by Lynden-Bell (1976); Lynden-Bell (1983) and Kunkel (1979) and calculated by Kroupa (1997) and Klessen & Kroupa (1998), which are based on observed properties of TDGs, thus lead to a population of ancient TDGs that are in reasonable agreement with the observed luminosities, dimensions, and M/L ratios of

dSph satellites (Metz & Kroupa 2007). These model-dSph satellites require no fine tuning of parameters but only assume the formation about 10 Gyr ago of about $10^7 M_{\odot}$ heavy TDGs composed purely of baryonic matter. This theoretical framework of satellite galaxies does not imply any relation between luminosity and (wrongly inferred) “dynamical mass”, in agreement with the lack of this relation (Sect. 2). And it would naturally explain why the mass function of luminous DM sub-halos cannot account for the observations (Sect. 3). Within Newtonian dynamics, this dynamical modelling over many orbits around the MW DM halo has demonstrated that even low-mass satellites do not easily disrupt unless they are on virtually radial orbits (Kroupa 1997; Metz & Kroupa 2007).

Summarising Sect. 6.1, the physics of TDG formation and evolution is sufficiently well understood to conclude that 1) *once formed at a sufficient distance from the host, TDGs will take an extremely long time to dissolve, if at all;* and 2) the TDGs formed will naturally lead to a population of ancient TDGs that resemble dSph satellites. A bulge-mass-number of satellite correlation and a DoS arise naturally in this scenario.

6.2. On the substructure problem

The MW dSph satellites can therefore be understood as ancient TDGs that formed within a DM universe. But on the other hand, the extensive modelling within the CCM strictly implies, if DM is cold or warm (but not hot), that MW-luminous galaxies must be accompanied by hundreds (with a slight dependence on the cold or warm nature of DM) of shining albeit faint satellites, which are not of tidal origin (Knebe et al. 2008; Macciò et al. 2010; Busha et al. 2010; Koposov et al. 2009). For example, Tollerud et al. (2008) conjecture that “there should be between 300 and 600 satellites within $D = 400$ kpc of the Sun that are brighter than the faintest known dwarf galaxies and that there may be as many as 1000, depending on assumptions.” Deep follow-up observations of the low S/N ultra-low-luminosity satellite candidates introduced by Walsh et al. (2009) show that these are not dSphs as a population. These results show that there is not a significant number of missing, ultra-low-luminosity satellites ($M_V > -2, D < 40$ kpc) in the SDSS footprint, i.e. an area covering half of the Northern hemisphere (Jerjen et al., in prep.). This may be a problem because of the Λ CDM prediction that there should be a dozen additional satellites ($M_V < 0, D < 40$ kpc) in a quarter celestial sphere (e.g. Fig. 4 in Koposov et al. 2009; see also Cooper et al. 2010).

If the dSph satellites are ancient TDGs stemming from an early gas-rich encounter involving the proto-MW and probably contributing a collision product to the MW bulge (see Sect. 4), then this would mean that the MW would have a severe substructure problem as there would not be any satellites with DM halos less massive than about $10^{10} M_{\odot}$ with stars, in conflict with DM predictions provided by, e.g., Knebe et al. (2008), Diemand et al. (2008), Busha et al. (2010), Macciò et al. (2010), and Koposov et al. (2009). Perhaps a few dSph satellites are ancient TDGs, such as the classical or nine brightest satellites, and the remainder are the DM dominated sub-halos? This possibility is unlikely, because the new satellites span the same DoS (Sect. 5.3) and because they do not form a population with physical properties that differ distinctly from those of the classical satellites (e.g. Strigari et al. 2008).

Summarising Sect. 6.2, based purely on the existence of the satellite phase-space correlation and the formation and survival of TDGs in a hierarchical structure formation framework the Fritz Zwicky Paradox emerges and the validity of the DM

hypothesis must be questioned, because the dSph satellites cannot be two types of object at the same time, namely DM-dominated sub-structures and ancient DM-free TDGs.

6.3. Early-type galaxies

But if TDGs account for the dSph satellites of the MW, would they then not also be an important population in other environments? The production of TDGs in the CCM has been calculated by Okazaki & Taniguchi (2000). Intriguingly, they find that TDGs naturally match the observed number of dE galaxies in various environments. The result of Okazaki & Taniguchi (2000) is rather striking, since they find that within the CCM framework only one to two long-lived (i.e., bright) TDGs need to be produced on average per gas-dissipational encounter to cater for the population of dwarf elliptical (dE) galaxies and for the density–morphology relation in the field, in galaxy groups and in clusters¹².

Viewing dE galaxies as old TDGs would be consistent with them deviating from the mass-radius, $M(r)$, relation of pressure-supported (early-type) stellar systems. The dE and dSph galaxies follow a $r \propto M^{1/3}$ sequence reminiscent of tidal-field-dominated formation. All other pressure-supported galactic systems (elliptical galaxies, bulges, and ultra-compact dwarf galaxies) with stellar mass $M > 10^6 M_\odot$ follow instead the relation $r \propto M^{0.60 \pm 0.01}$ (see Fig. 2 in Dabringhausen et al. 2008, see also Fig. 7 in Forbes et al. 2008 and Fig. 11 in Graham & Worley 2008), which may result from opacity-limited monolithic collapse (Murray 2009). Viewing dE galaxies as TDGs would also be consistent with the observation that they have essentially stellar mass-to-light ratios similar to globular clusters (Bender et al. 1992; Geha et al. 2003; Dabringhausen et al. 2008; Forbes et al. 2008). If dE (baryonic mass $> 10^8 M_\odot$) and dSph (baryonic mass $< 10^8 M_\odot$) galaxies are old TDGs, why do they appear as different objects? That the dE and dSph galaxies differ in terms of their baryonic-matter density may be a result of the finding that below $10^8 M_\odot$ spheroidal objects on the $r \propto M^{1/3}$ relation cannot hold their warm gas and consequently they must expand (Pflamm-Altenburg & Kroupa 2009a), becoming more susceptible to tides from their host.

dE galaxies are pressure-supported stellar systems, while young TDGs are rotationally supported (Bournaud et al. 2008). With a mass of less than typically $10^9 M_\odot$, the velocity dispersion of their stellar populations becomes comparable to their rotational velocity (of the order of 30 km s^{-1}). That a sizeable fraction of dE galaxies show rotation, some even with spiral structure (Jerjen et al. 2000; Barazza et al. 2002; Geha et al. 2003; Ferrarese et al. 2006; Chilingarian 2009; Beasley et al. 2009), is thus also consistent with their origin as TDGs. For an excellent review on dE galaxies the reader is referred to Lisker (2009).

One is thus led to the following seemingly logical impasse, i.e. to the Fritz Zwicky Paradox. In the CCM, TDGs are formed and their number and distribution is calculated to match the number and distribution of observed dE galaxies in the different environments. Within the CCM, the observed luminous dwarf

¹² Note that Okazaki & Taniguchi (2000) write: “Adopting the galaxy interaction scenario proposed by Silk & Norman, we find that if only a few dwarf galaxies are formed in each galaxy collision, we are able to explain the observed morphology–density relations for both dwarf and giant galaxies in the field, groups of galaxies, and clusters of galaxies.” They also state “The formation rate of TDGs is estimated to be $\sim 1\text{--}2$ in each galaxy interaction.” and proceed to compare this number with the actually observed number of TDGs born in galaxy encounters. This statement is at odds with the quotation in Bournaud (2010).

sub-structures are thus naturally accounted for by TDGs. But the dE galaxies cannot be both, DM sub-halos *and* TDGs at the same time.

Summarising Sect. 6.3, the physical processes at play during structure formation in the CCM imply that dE galaxies ought to be identified as ancient TDGs. Thus, there would be no room for shining DM substructures.

6.4. Deeper implications: gravitational dynamics

In Sects. 6.2 and 6.3 it has been shown that the DM hypothesis leads to the Fritz Zwicky Paradox when accounting for the number of satellite and dE galaxies because the formation of TDGs is an intrinsic outcome of structure formation. In Sects. 2 to 5 it has also been shown that the CCM seems to have a rather major problem accounting for the observed Galactic satellites and their internal properties. This situation suggests that alternative ideas should be considered to help us understand the origin of these problems, and indeed repeat the steps that had led to a full-fledged DM framework of structure formation but with a different outlook. Since structure formation in the DM framework relies on Newtonian gravitation in the weak-field limit, one is naturally led to relax insistence on Newtonian dynamics in the weak-field limit and to consider modified gravitation theories, which remain compatible with General Relativity in the strong field regime and with the observed large-scale structure. We note that adopting non-Newtonian dynamics in the weak-field limit would *not* necessarily rule out the existence of DM: on the scale of galaxy clusters DM might still be needed, but instead of being warm or cold, it would be *hot* (Angus et al. 2009).

6.4.1. Non-Newtonian weak-field gravity

Alternatives to Newtonian dynamics in the weak-field limit have been studied in great detail. The increasingly popular modified-Newtonian-dynamics (MOND) approach rests on a modification of the Newtonian acceleration in the weak-field limit, i.e. when the Newtonian acceleration a is smaller than a threshold a_0 (Milgrom 1983; Bekenstein & Milgrom 1984; Sanders & McGaugh 2002; Bekenstein 2004; Famaey & Binney 2005; Famaey et al. 2007; Sanders 2007, 2008; McGaugh 2008; Nipoti et al. 2008; Tiret & Combes 2008; Bruneton et al. 2009). A modified-gravity (MOG) adding a Yukawa-like force in the weak-field limit has also been under investigation (Moffat & Toth 2009a; Moffat & Toth 2009b, and references therein). In addition, an extension of the General Theory of Relativity to a class of alternative theories of gravity without DM and based on generic functions $f(R)$ of the Ricci scalar curvature R have been developed and successfully applied to the problem of galactic rotation curves (e.g. Capozziello et al. 2009). For a brief review of MOND and MOG and Milgrom’s proposition on the possible physical origin for the existence of a_0 , the reader is directed to the Appendix.

Both the MOND and MOG approaches have been applied to the satellite galaxy problem with appreciable success (Milgrom 1995; Brada & Milgrom 2000; Angus 2008; Moffat & Toth 2008; Hernandez et al. 2010; McGaugh & Wolf 2010). It has already been conclusively demonstrated that spiral galaxy rotation curves are well recovered in MOND purely by the baryon distribution without any parameter adjustments (Sanders & McGaugh 2002; McGaugh 2004, 2005a; Sanders & Noordermeer 2007), and MOG is reported to also do well on this account (Brownstein & Moffat 2006). In contrast, the DM approach can only poorly

reproduce the vast variety of rotation curves, and cannot explain the amazing regularities found in them (McGaugh 2004; McGaugh et al. 2007; Gentile et al. 2009; Milgrom 2009a). Notably, the realisation (Gentile et al. 2009; Milgrom 2009a) that the ratio of DM mass to baryonic mass within the DM core radius is constant despite the large variation in the DM-to-baryonic-matter ratio globally within galaxies cannot be understood within the DM hypothesis. A constant ratio within that radius implies that the distribution of baryonic matter is indistinguishable from that of the supposedly present DM (as already found by Bosma 1981). This implies a hitherto not predicted near-exact coupling between DM and baryonic matter that does not arise naturally in the CCM, while outside that radius the effects of DM should become noticeable (McGaugh 2010). The only way to physically couple DM and baryons with each other to this degree would be by postulating the existence of an unknown dark force that acts only between DM particles and baryons. The modified DM cosmology would then comprise inflation, dark matter, a dark force, and dark energy.

In MOND models, this behaviour of gravity comes naturally. That the rotation curves would be purely defined by the baryonic matter distribution in non-DM models indeed would naturally explain the later finding based on a large sample of galaxies by Disney et al. (2008), Gentile et al. (2009), and Milgrom (2009a) that disc galaxies appear to be governed by a single parameter. Furthermore, the high galaxy-cluster-galaxy-cluster velocities required to obtain the features of the Bullet cluster have been shown to be extremely unlikely in the CCM (Sect. 1), but these velocities are found to naturally occur in MOND (Angus & McGaugh 2008). Last but not least, the *time-delay problem* of the CCM mentioned in Sect. 1 would disappear naturally.

6.4.2. A consistency check

If it were true that the physical Universe is non-Newtonian in the weak-field limit, then a simple test would provide a consistency check: high dynamical mass-to-light ratios, $(M/L)_{\text{dyn}}$, (derived assuming Newtonian dynamics) would not be due to DM but due to the dynamics being non-Newtonian in the weak-field limit and/or be due to objects being unbound non-equilibrium systems (Sect. 6.1). Thus, taking MOND to be a proxy for non-Newtonian dynamics in the weak-field limit (MOND is, arguably, the currently available simplest alternative to Newtonian dynamics in the weak-field limit), all systems with non-stellar $(M/L)_{\text{dyn}}$ values (as derived in Newtonian gravity) would have to have internal accelerations roughly below the MONDian value¹³ $a_0 = 3.9 \text{ pc/Myr}^2$. That is, all pressure-supported (spheroidal) stellar systems that appear to be dominated dynamically by DM would need to have an internal acceleration $a < a_0$. Note that the emphasis here is on pressure-supported systems since rotationally supported systems have been extensively and successfully studied in non-Newtonian gravitational theories and because dSph and dE galaxies are mostly pressure-supported objects.

Figure 7 shows the acceleration,

$$a(r_e) = G \frac{M}{r_e^2} = G \frac{0.5\Upsilon \cdot L_V}{r_e^2}, \quad (18)$$

that a star inside a pressure-supported system experiences at the effective radius, r_e , of its host system with luminosity spanning

¹³ Note that this statement is approximately true for all non-Newtonian gravitational theories since they must account for the same non-Newtonian phenomena in the weak-field limit.

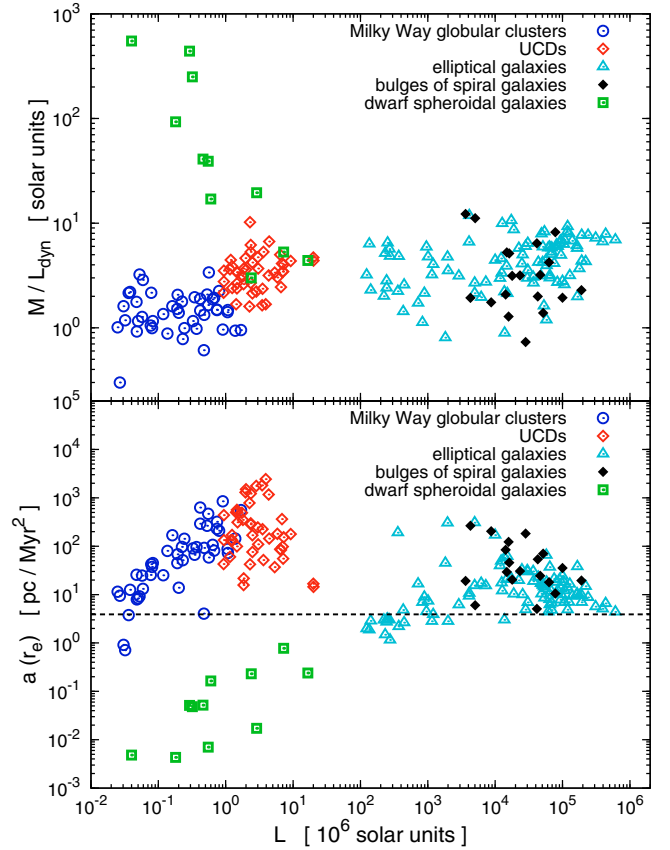


Fig. 7. *Upper panel:* the dynamical $(M/L)_{\text{dyn}}$ ratio (calculated assuming Newtonian dynamics to be valid in the weak-field limit) in dependence of the luminosity, L_V , for pressure-supported stellar systems following Dabringhausen et al. (2008). Note that here dE ($<10^{10} L_\odot$) and E ($>10^{10} L_\odot$) galaxies are both plotted with the same symbol. *Lower panel:* the Newtonian acceleration (Eq. (18)) of a star located at the effective radius within the host system in dependence of the host luminosity. The dashed line is a_0 . Note that M/L_{dyn} is high in pressure-supported stellar systems only when $a < a_0$. In both panels: UCD = ultra compact dwarf galaxy. Comparing the upper and lower panels shows that evidence of DM ($M/L_{\text{dyn}} > 10$) appears only when $a < a_0$.

10^4 to $10^{12} L_\odot$. Here $M = 0.5\Upsilon L_V$ is the stellar mass within r_e and L_V is the absolute V-band luminosity in solar units. The stellar mass-to-light ratio in the V-band is $\Upsilon \approx 3$ for collisionless systems (two-body relaxation time longer than a Hubble time), while $\Upsilon \approx 1.5$ for collisional systems, i.e. for systems that have evaporated a significant fraction of their faint low-mass stars by means of energy equipartition (Kruijssen & Lamers 2008; Kruijssen & Mieske 2009). Values of $(M/L)_{\text{dyn}}$ as high as 10 can be expected for purely baryonic systems if these retain their stellar remnants and hot gas. For example, the mass of an E galaxy may be comprised of only 30 per cent or less of stars, the rest consisting of stellar remnants and gas that cannot cool to form new stars (Parriott & Bregman 2008; Dabringhausen et al. 2009), meaning that $\Upsilon = 5$ would be an underestimate in that case. Ultra-compact dwarf galaxies, UCDs (sometimes also understood as extremely massive star clusters), have high stellar M/L values perhaps due to a bottom-heavy IMF (Mieske & Kroupa 2008) or a top-heavy IMF (Dabringhausen et al. 2009).

By comparing the two panels in Fig. 7, it is indeed evident that only those systems with $a < a_0$ show non-baryonic $(M/L)_{\text{dyn}}$ values. This is more clearly shown in Fig. 8 where the MOND

prediction for the range of dynamical mass-to-light ratios measured by a Newtonist living in a MONDian universe is plotted as a function of Newtonian acceleration. For this figure, the MOND expectation for the mass-to-light ratio, which an observer who thinks to live in a Newtonian world would deduce, was calculated as follows. Adopting a conservative value of the baryonic mass-to-light ratio Υ_{bar} between 0.7 (for a globular cluster with an old metal-poor population depleted in low-mass stars) and 5 (for an old metal-rich population), the prediction of MOND inside the effective radius is (Famaey & Binney 2005; Angus et al. 2009)

$$(M/L)_{\text{dyn mond}} = 0.5 \times \Upsilon_{\text{bar}} \times \left(1 + \sqrt{1 + 4a_0/a}\right). \quad (19)$$

We note that, writing customarily $x = g/a_0$, where g is the actual full acceleration experienced by a ballistic particle (in MOND)¹⁴, Eq. (19) follows from the form of the transition MOND function (Milgrom 1983)

$$\mu(x) = x/(1 + x), \quad (20)$$

which is valid up to $x \approx 10$. The theoretical transition derived by Milgrom (1999) and mentioned in the Appendix would yield virtually the same result.

The three classical dwarfs that lie outside the predicted MOND range for $(M/L)_{\text{dyn}}$ in Fig. 8 are UMa, Draco, and UMi. UMa may have an anisotropic velocity dispersion (Angus 2008); Draco is known to be a long-standing problem for MOND, but the technique of interloper removal developed by Serra et al. (2009) could probably solve the problem, although this particular case remains open to debate; UMi is a typical example of a possibly out-of-equilibrium system, as it is elongated with substructure and shows evidence of tidal tails (Martinez-Delgado, priv. communication). Ultra-faint dwarf spheroidals are expected to be increasingly affected by this kind of non-equilibrium dynamics, as shown to be true even for Newtonian weak-field dynamics (Kroupa 1997, Sect. 6.1), and even more strongly so in MOND (McGaugh & Wolf 2010).

To conclude this subsection, well-developed non-Newtonian weak-field approaches exist and have been shown to account for galaxy properties much more successfully than the CCM, which would need to be extended by a dark force to account for the observed strong coupling between DM and baryons. All known pressure-supported stellar systems ranging from elliptical to dwarf satellite galaxies behave dynamically as expected in a MONDian universe. In DM cosmology, the association of highly non-stellar $(M/L)_{\text{dyn}}$ values with $a < a_0$ would be coincidental as it is not built into the theory. It is, however, natural in a MONDian universe for observers who interpret weak-field observations with Newtonian dynamics.

7. Conclusions and perspectives

We inhabit a Universe for which physicists seek mathematical formulations. A successful formulation of gravitational physics, the General Theory of Relativity (GR), requires the existence of non-baryonic dark matter (DM) in order to account for the observed rotation curves of galaxies and other dynamical effects in this theory, which has Newtonian dynamics as its weak-field limit. On the other hand, non-Newtonian weak-field gravitational theories have also been formulated to account for the ‘‘DM-effects’’ observed in galaxies.

¹⁴ In the notation applied here, the MOND formula becomes $a = \mu(x)g$, where the Newtonian acceleration a is given by Eq. (18).

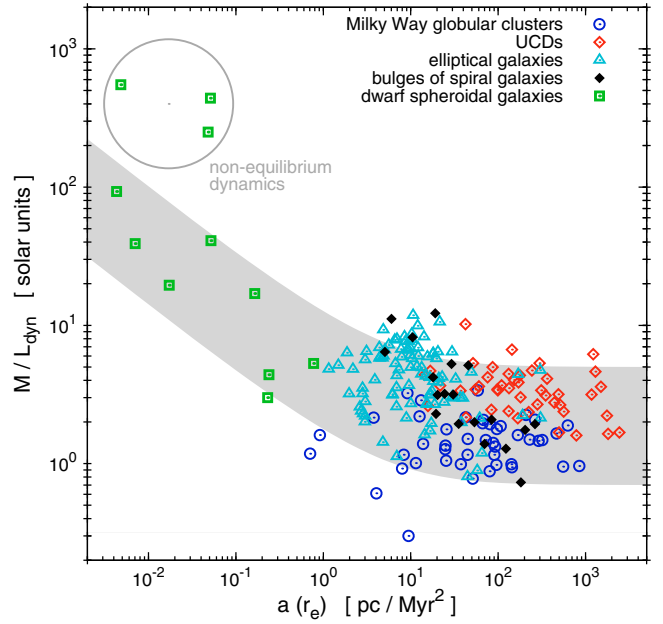


Fig. 8. The correlation between the acceleration $a(r_e)$ and the dynamical mass-luminosity ratio $(M/L)_{\text{dyn}}$ derived assuming Newtonian dynamics is shown for the same objects as in Fig. 7. The shaded region indicates the range in $(M/L)_{\text{dyn}}$ as it follows directly from MOND models (without any parameter adjustments) using Eq. (19). The graph shows the consistency of the data in a MONDian universe for an observer who interprets observations with Newtonian dynamics. Encircled dwarf spheroidals outside this range (UMa, Dra, and UMi) may indicate non-equilibrium dynamics, either because the whole system is unbound, or because of unbound interloper stars among the member stars (see Sect. 6.4.2). That virtually all pressure-supported stellar systems fall in the shaded MOND region suggests a successful consistency check. That is, stellar dynamics is MONDian rather than Newtonian on galactic scales.

Finding a definitive test that distinguishes between these two different solutions to the problem of galactic dynamics and cosmological structure formation is difficult. Both DM and modified gravity are designed to solve similar problems, so the test must rely on subtle differences between the models and the observational data. Thus far, GR+DM+ Λ +inflation (the CCM) accounts for the emergence of structure on large scales, and Reyes et al. (2010) were able to exclude certain versions of alternative gravitational theories that had already been known by the respective community to be unstable (Contaldi et al. 2008). But, as shown here, the CCM appears to have insurmountable problems on galaxy scales such that other alternative approaches need to be studied. A speculative ansatz to perhaps solve the observed near-exact DM-baryon coupling in galaxies within a DM-Newtonian cosmology would be to extend the CCM by postulating the existence of a *dark force* (DF) leading to a GR+DM+DF+ Λ +inflation cosmology that should perhaps be investigated in more detail in the future. The greatest differences between the two competing approaches (CCM versus non-Newtonian dynamics in the weak-field limit) are expected in the weak gravitational regime where the subtleties of non-Newtonian weak-field dynamics are most pronounced, which is why the constituents of the outer edges of galaxies allow the most stringent tests.

This contribution has statistically assessed whether the observed properties of satellite galaxies in the Local Group, which

are the result of structure formation in the weak-field limit, are consistent with the CCM. Given that a substantial number of independent research groups working in the traditional CDM and WDM approaches have by now made firm statements about the dwarf satellite galaxies of the MW and Andromeda such that the missing satellite problem is deemed to be solved, the CCM can be further tested sensitively on these scales within the Local Group.

Five new problems for the CCM on the scale of the Local Group and dwarf galaxies have been uncovered: (i) the observed absence of a mass-luminosity relation (Sect. 2, the *DM-mass-luminosity problem*); (ii) the mass function of luminous galactic satellites (Sect. 3, the *mass function of luminous satellite problem*); (iii) the observed relation between the bulge mass and the number of satellites (Sect. 4, the *bulge-satellite correlation problem*); (iv) the accordance with the Milky Way’s disc-of-satellites of the recently detected ultra-faint dwarfs (Sect. 5, the *phase-space correlation problem*); and (v) the low probability that two neighbouring MW-type DM halos contain similar MW-type disk galaxies (Sect. 5.5, the *invariant-baryonic-galaxy problem*).

It is found that the CCM is consistent with the Local Group data with a combined probability¹⁵ $p \ll 3 \times 10^{-3}$. The five problems thus appear to rather strongly challenge the notion that the CCM successfully accounts for galactic structure in conflict with a vast volume of reported research (compare with Fanelli 2010). All these challenges constitute a strong motivation for numerous future observational and theoretical investigations. For instance, the disk of satellites will have to be confirmed by surveys such as Pan-Starrs (Burgett & Kaiser 2009) and the Stromlo Milky Way Satellite Survey (SMS) (Jerjen 2010). Given the existence of the DoS and by symmetry, the southern hemisphere ought to also contain about 16 satellites, such that the SMS survey is expected to discover about 8 new southern satellites (Fig. 4). It will also be essential to refine the correlation between bulge-mass and satellite-number with extragalactic surveys. On the theoretical side, more inclusive modelling is needed to address these challenges within the CCM while, at the same time, existing viable alternatives should be further explored.

With this contribution, the following clues have emerged suggesting the need for a new scenario for the origin and nature of dSph satellite galaxies. The observed correlation between bulge mass and number of satellites suggests that a link between these two quantities may exist. The phase-space correlation of the classical and ultra-faint satellite galaxies implies that angular momentum conservation played an important role in establishing the satellite distribution. Given that bulges form in dissipational encounters, during which angular-momentum conservation rearranges matter on Galactic scales to be in highly correlated phase-space structures (tidal arms), a natural path thus opens to understand the likely origin of satellite galaxies. Already in the 1970’s a tidal origin for dwarf spheroidal galaxies was suggested, based on their arrangement around the Milky Way (Sect. 6). This solution does imply, however, that the dSph galaxies are ancient TDGs and not DM sub-haloes. Furthermore, by logical implication, dE galaxies would also

be TDGs (Sect. 6.3). This would imply that the vast majority of $\lesssim 10^{10} M_{\odot}$ DM sub-halos are unable to make stars. This, however, would be in conflict with all the CCM computations available to date *to the extent that the CCM would have to be discarded in favour of a universe without cold or warm DM*. In this case, the non-Keplerian rotation curves of galaxies and other DM effects additionally suggest that we live in a non-Newtonian weak-field framework within which galaxies would be pure baryonic objects¹⁶.

This scenario would naturally solve problems (iii) and (iv), while it would not imply a “dynamical mass”-luminosity relation if the dwarfs are out of equilibrium, so could possibly solve problem (i). For purely baryonic galaxies, problem (ii) would not exist anymore by definition. Problem (v) would also vanish naturally. What is more, while in the CCM the association of highly non-stellar $(M/L)_{\text{dyn}}$ values with $a < a_0$ would be coincidental because it is not built into the theory, it is natural in a non-Newtonian universe for weak-field observers who interpret observations with Newtonian dynamics. Noteworthy is that the same statement can be made for the Tully-Fisher scaling relation for rotationally-supported galaxies (Tully & Fisher 1977; McGaugh 2005b; Combes 2009a) as well as the newly found scaling relation of Gentile et al. (2009) and Milgrom (2009a). The supposed mass-deficit seen in young rotating and gaseous TDGs (such as those of NGC 5291) constitutes independent empirical evidence towards this same statement. Young tidal dwarf galaxies (TDG), which should be devoid of collisionless DM, appear to nevertheless exhibit a mass-discrepancy in Newtonian dynamics. This is a significant problem for the DM hypothesis, but it is naturally explained by MOND (Gentile et al. 2007; Milgrom 2007). Also, while the high Bullet-cluster velocity is hard to account for in the CCM, it is natural in MOND (Sects. 1, 6.4 and 6.4.1). And, it has already been noted by Sanders (1999) that the dynamical-mass – baryon-mass discrepancy observed in galaxy clusters is nearly removed in MONDian dynamics.

It would thus appear that within the non-Newtonian weak-field framework a much more complete, self-consistent, and indeed simpler understanding of the Galaxy’s satellites as well as of major galaxies may be attained, than within the CCM.

However, to affirm this statement, this alternative cosmological scenario will have to be investigated in as much detail as is now available for the CCM in order to perform equivalent tests as presented here for the DM hypothesis and to ascertain which of the non-Newtonian weak-field dynamics theories (and which versions of the theories) can most successfully account for the physical world. Models of merging gas-rich disc galaxies need to be computed in MOND, for example, to study how the formation of TDGs proceeds and how the number of satellites thus formed correlates with the bulge that forms as a result of the encounter. These populations of satellites associated with globular clusters that formed along with them would naturally appear in (more than one) closely related planes explaining the Lynden-Bell & Lynden-Bell (1995) streams, because a gas-rich galaxy pair undergoes many close encounters in MOND, each spawning some TDGs and globular clusters, before perhaps finally merging.

Figure 9 schematically depicts the structure formation scenario in this non-Newtonian weak-field framework: while purely baryonic galaxies would merge, these events would spawn dwarf

¹⁵ Summarising the likelihoods, p , that the CCM accounts for the observed data in the Local Group are in the individual tests: (1) mass-luminosity data: $p_1 < 0.3$ per cent (Sect. 2); (2) mass function of luminous sub-halos: $p_2 < 4.5$ per cent (Sect. 3); (3) bulge-satellite number: $p_3 \approx 4.4$ per cent (Sect. 4); (4) a MW-type galaxy with at least 11 satellites in a DoS: $p_4 = 0.4$ per cent; (5) a M31-type galaxy with at least 11 satellites: $p_5 = 1.4$ per cent (Sect. 5.4). Thus, the combined probability that the general CCM framework accounts for the Local Group is $p \ll 3 \times 10^{-3}$.

¹⁶ Given that Newton derived the gravitational $1/r^2$ law over a very limited physical range (Solar System), while with the Local Group gravitational physics is probed on a length scale nearly eight orders of magnitude larger and in a much weaker field regime, it need not be surprising that an adjusted gravitational law is needed.



Fig. 9. A new cosmological structure formation framework: the man-grove merger tree. In a modified-Newtonian weak-field framework, purely baryonic galaxies merge thereby spawning new dwarf galaxies giving rise to the morphology-density relation (adapted from Metz 2008).

galaxies such that a density–morphology relation would be established (more dE galaxies in denser environments, Okazaki & Taniguchi 2000).

The MONDian modelling by Tiret & Combes (2008) and Combes & Tiret (2009) has already shown that TDGs are produced during gas-dissipational galaxy mergers, and that the interaction times between galaxies are much longer, while the number of mergers is smaller than in a DM universe. Hence, the number of observed galaxy encounters would be given foremost by the long time scale of merging and thus by more close galaxy-galaxy encounters per merging event rather than on a high number of mergers.

This would imply that compact galaxy groups do not evolve statistically over more than a crossing time. In contrast, assuming DM-Newtonian dynamics to hold, the merging time scale would be about one crossing time because of dynamical friction in the DM halos such that compact galaxy groups ought to undergo significant merging over a crossing time. The lack of significant evolution of compact groups, if verified observationally, would appear not to be explainable if DM dominates galaxy dynamics. Analyses of well-studied compact groups indeed indicate this to be the case (Presotto et al. 2010).

Thus, many observational problems may be solved unconstrained by adopting non-Newtonian weak-field dynamics, and perhaps this was, in the end, the most self evident explanation to the discovery of non-Keplerian rotation curves by Rubin & Ford (1970)¹⁷.

¹⁷ On 19 June 2009, the final day of the conference “Unveiling the Mass: Extracting and Interpreting Galaxy Masses” in Kingston, Ontario, in honour of the career of Vera Rubin, PK asked her whether she would be very dismayed if her discovery that galaxies have non-Keplerian rotation curves would not be due to dark matter but rather non-Newtonian weak-field dynamics. Prof. Rubin replied that she would in fact be delighted, since the non-Keplerian rotation curves are an empirical observation of hitherto not understood physics, and one needs to keep an open mind in seeking solutions.

Acknowledgements. This work was supported by the Alexander von Humboldt Foundation (BF), and by the German Research Foundation (DFG) through grants KR1635/18-1 and HE1487/36-2 within the priority programme 1177 “Witnesses of Cosmic History: Formation and Evolution of Black Holes, Galaxies and Their Environment”, and a grant from the DAAD-Go8 Germany Australia Joint Research co-operative scheme. We acknowledge useful discussions with Iskren Georgiev, Anton Ippendorf, Antonino Del Popolo and Beth Willman. We thank Jelte de Jong for allowing us to use the image from Coleman et al. (2007a) in our Fig. 6.

Appendix A: Brief review of MOND and MOG and Milgrom’s proposition on the possible physical origin and value of a_0

Theoretical approaches trying to embed MOND within a Lorentz-covariant framework (Bekenstein 2004; Sanders 2005; Zlosnik et al. 2007; Zhao 2008; Bruneton & Esposito-Farèse 2008; Blanchet & Le Tiec 2009; Esposito-Farèse 2009; Skordis 2009; Milgrom 2009b) are currently under intense scrutiny, and a quasi-linear formulation of MOND has been discovered only recently (Milgrom 2010; Zhao & Famaey 2010), which appears to allow easier access to N-body calculations.

However, none of these theories is (yet) fully satisfactory from a fundamental point of view (see e.g. Contaldi et al. 2008; Bruneton & Esposito-Farèse 2008; Reyes et al. 2010) and moreover none of them explains (yet) why the acceleration threshold, a_0 , which is the single parameter of MOND (adjusted by fitting to one single system), is about $c\sqrt{\Lambda/3}$ (where Λ is the cosmological constant and c the speed of light), or that $a_0 \approx cH_0/2\pi$, where H_0 is the current Hubble constant. They also require a transition function, $\mu(x)$ (e.g. Eq. (20)), from the Newtonian to the modified regime, a function not (yet) rooted in the theory.

A possible explanation of the coincidence $a_0 \approx c\sqrt{\Lambda/3}$ and a theoretically-based transition function are suggested by Milgrom (1999). In Minkowski (flat) space-time, an accelerated observer sees the vacuum as a thermal bath with a temperature proportional to the observer’s acceleration (Unruh 1975). This means that the inertial force in Newton’s second law can be defined to be proportional to the Unruh temperature. On the other hand, an accelerated observer in a de Sitter universe (curved with a positive cosmological constant Λ) sees a non-linear combination of the Unruh (1975) vacuum radiation and of the Gibbons & Hawking (1977) radiation due to the cosmological horizon in the presence of a positive Λ . Milgrom (1999) then defines inertia as a force driving such an observer back to equilibrium as regards the vacuum radiation (i.e. experiencing only the Gibbons-Hawking radiation seen by a non-accelerated observer). Observers experiencing a very small acceleration would thus see an Unruh radiation with a low temperature close to the Gibbons-Hawking one, meaning that the inertial resistance defined by the difference between the two radiation temperatures would be smaller than in Newtonian dynamics, and thus the corresponding acceleration would be larger. This is given precisely by the MOND formula of Milgrom (1983) with a well-defined transition-function $\mu(x)$, and $a_0 = c(\Lambda/3)^{1/2}$. Unfortunately, no covariant version (if at all possible) of this approach has been developed yet.

The theoretical basis of the MOG approach relies on chosen values of integration constants in solving the equations of the theory. This approach seems to work well from an observational point of view, but its fundamental basis needs further research, as is also the case for MOND. It is noteworthy that a formulation of MOG in terms of scalar, vector, and tensor fields (Moffat 2006) may possibly hint at a convergence with the Bekenstein (2004) tensor-vector-scalar theory of gravity.

References

- Adén, D., Feltzing, S., Koch, A., et al. 2009a, *A&A*, 506, 1147
- Adén, D., Wilkinson, M. I., Read, J. I., Feltzing, S., et al. 2009b, *ApJ*, 706, L150
- Angus, G. W. 2008, *MNRAS*, 387, 1481
- Angus, G. W., & McGaugh, S. S. 2008, *MNRAS*, 383, 417
- Angus, G. W., Famaey, B., & Diaferio, A. 2009, *MNRAS*, 1871
- Aubert, D., Pichon, C., & Colombi, S. 2004, *MNRAS*, 352, 376
- Barazza, F. D., Binggeli, B., & Erjen, H. 2002, *A&A*, 391, 823
- Barnes, J. E., & Hernquist, L. 1992, *Nature*, 360, 715
- Beasley, M. A., Cenarro, A. J., Strader, J., & Brodie, J. P. 2009, *AJ*, 137, 5146
- Bekenstein, J., & Milgrom, M. 1984, *ApJ*, 286, 7
- Bekenstein, J. D. 2004, *Phys. Rev. D*, 70, 083509
- Belokurov, V., Zucker, D. B., Evans, N. W., et al. 2006, *ApJ*, 647, L111
- Belokurov, V., Zucker, D. B., Evans, N. W., et al. 2007, *ApJ*, 654, 897
- Belokurov, V., Walker, M. G., Evans, N. W., et al. 2008, *ApJ*, 686, L83
- Belokurov, V., Walker, M. G., Evans, N. W., et al. 2009, *MNRAS*, 397, 1748
- Belokurov, V., Walker, M. G., Evans, N. W., et al. 2010, *ApJ*, 712, L103
- Bender, R., Burstein, D., & Faber, S. M. 1992, *ApJ*, 399, 462
- Bertone, G., Hooper, D., & Silk, J. 2005, *Phys. Rep.*, 405, 279
- Blanchet, L., & Le Tiec, A. 2009, *Phys. Rev. D*, 80, 023524
- Blumenthal, G. R., Faber, S. M., Primack, J. R., & Rees, M. J. 1984, *Nature*, 311, 517
- Boily, C. M., Nakasato, N., Spurzem, R., & Tsuchiya, T. 2004, *ApJ*, 614, 26
- Bosma, A. 1981, *AJ*, 86, 1791
- Bosma, A., Goss, W. M., & Allen, R. J. 1981, *A&A*, 93, 106
- Bournaud, F. 2010, *Adv. Astron.*, 2010, 1
- Bournaud, F., Duc, P.-A., Brinks, E., et al. 2007, *Science*, 316, 1166
- Bournaud, F., Duc, P.-A., & Emsellem, E. 2008, *MNRAS*, 389, L8
- Brada, R., & Milgrom, M. 2000, *ApJ*, 541, 556
- Brownstein, J. R., & Moffat, J. W. 2006, *ApJ*, 636, 721
- Bruneton, J.-P., & Esposito-Farèse, G. 2008, *Phys. Rev. D*, 76, 124012
- Bruneton, J.-P., Liberati, S., Sindoni, L., & Famaey, B. 2009, *J. Cosmol. Astro-Part. Phys.*, 3, 21
- Bullock, J. S., Kolatt, T. S., Sigad, Y., et al. 2001, *MNRAS*, 321, 559
- Burgett, W., & Kaiser, N. 2009, *Proceedings of the Advanced Maui Optical and Space Surveillance Technologies Conference*, held in Wailea, Maui, Hawaii, September 1–4, ed. S. Ryan, The Maui Economic Development Board., E39
- Busha, M. T., Alvarez, M. A., Wechsler, R. H., Abel, T., & Strigari, L. E. 2010, *ApJ*, 710, 408
- Capozziello, S., Piedipalumbo, E., Rubano, C., & Scudellaro, P. 2009, *A&A*, 505, 21
- Chilingarian, I. V. 2009, *MNRAS*, 394, 1229
- Cole, S., Percival, W. J., Peacock, J. A., et al. 2005, *MNRAS*, 362, 505
- Coleman, M. G., de Jong, J. T. A., Martin, N. F., et al. 2007a, *ApJ*, 668, L43
- Coleman, M. G., Jordi, K., Rix, H.-W., Grebel, E. K., & Koch, A. 2007b, *AJ*, 134, 1938
- Combes, F. 2009a, *A&A*, 500, 119
- Combes, F. 2009b, 4 pages, *Concluding remarks in Galaxies in isolation: exploring Nature vs. Nurture* (May 2009, Granada, Spain) [arXiv:0909.2752]
- Combes, F., & Tiret, O. 2009, in *The Invisible Universe*, ed. J.-M. Alimi, A. Fuzfa, P.-S. Corasaniti, AIP, eprint [arXiv:0908.3289]
- Contaldi, C. R., Wiseman, T., & Withers, B. 2008, *Phys. Rev. D*, 78, 044034
- Cooper, A. P., Cole, S., Frenk, C. S., et al. 2010, *MNRAS*, 406, 744
- Clowe, D., Bradač, M., Gonzalez, A. H., et al. 2006, *ApJ*, 648, L109
- Dabringhausen, J., Hilker, M., & Kroupa, P. 2008, *MNRAS*, 386, 864
- Dabringhausen, J., Kroupa, P., & Baumgardt, H. 2009, *MNRAS*, 394, 1529
- Dall’Ora, M., Clementini, G., Kinemuchi, K., et al. 2006, *ApJ*, 653, L109
- de Jong, J. T. A., Rix, H.-W., Martin, N. F., et al. 2008, *AJ*, 135, 1361
- de Jong, J. T. A., Martin, N. F., Rix, H.-W., et al. 2010, *ApJ*, 710, 1664
- Dekel, A., & Silk, J. 1986, *ApJ*, 303, 39
- Dekel, A., & Woo, J. 2003, *MNRAS*, 344, 1131
- Del Popolo, A., & Yesilyurt, I. S. 2007, *Astron. Rep.*, 51, 709
- Demleitner, M., Accomazzi, A., Eichhorn, G., Grant, C. S., et al. 2001, in *Astronomical Data Analysis Software and Systems X*, ed. F. R. Harnden, Jr., A. P. Francis, & E. P. Harry (San Francisco: ASP, ASP Conf. Proc.), 238, 321
- Diemand, J., Kuhlen, M., Madau, P., et al. 2008, *Nature*, 454, 735
- Disney, M. J., Romano, J. D., Garcia-Appadoo, D. A., et al. 2008, *Nature*, 455, 1082
- D’Onghia, E., & Lake, G. 2008, *ApJ*, 686, L61
- Einstein, A. 1921, *Festschrift der Kaiser-Wilhelm Gesellschaft zur Förderung der Wissenschaften zu ihrem zehnjährigen Jubiläum dargebracht von ihren Instituten* (Berlin: Springer), 50
- Esposito-Farèse, G. 2009, *lecture given at the School on Mass*, Orleans, France, June 2008, eprint [arXiv:0905.2575]
- Fanelli, D. 2010, *PLoS ONE* 5(4): e10271
- Famaey, B., & Binney, J. 2005, *MNRAS*, 363, 603
- Famaey, B., Gentile, G., Bruneton, J.-P., & Zhao, H. S. 2007, *Phys. Rev. D*, 75, 063002
- Fellhauer, M., Belokurov, V., Evans, N. W., et al. 2006, *ApJ*, 651, 167
- Ferrarese, L., Cote, P., Jordan, A., et al. 2006, *ApJS*, 164, 334
- Forbes, D. A., Lasky, P., Graham, A. W., & Spitler, L. 2008, *MNRAS*, 389, 1924
- Gao, L., White, S. D. M., Jenkins, A., Stoehr, F., & Springel, V. 2004, *MNRAS*, 355, 819
- Gavazzi, G. 2009, *Rev. Mex. Astron. Astrofis. Conf. Ser.*, 37, 72
- Gebhardt, K., Lauer, T. R., Kormendy, J., et al. 2001, *AJ*, 122, 2469
- Geha, M., Guhathakurta, P., & van der Marel, R. P. 2003, *AJ*, 126, 1794
- Geha, M., Willman, B., Simon, J. D., et al. 2009, *ApJ*, 692, 1464
- Gentile, G., Famaey, B., Combes, F., et al. 2007, *A&A*, 472, L25
- Gentile, G., Famaey, B., Zhao, H., & Salucci, P. 2009, *Nature*, 461, 627
- Gibbons, G. W., & Hawking, S. W. 1977, *Phys. Rev. D*, 15, 2738
- Gilmore, G., Wilkinson, M. I., Wyse, R. F. G., et al. 2007, *ApJ*, 663, 948
- Graham, A. W., & Worley, C. C. 2008, *MNRAS*, 388, 1708
- Grebel, E. K. 1999, in *The Stellar Content of Local Group Galaxies*, ed. P. Whitelock, & R. Cannon, IAU Symp., 192, 17
- Grebel, E. K. 2008, *Baryonic Properties of the Darkest Galaxies*, in *Dark Galaxies and Lost Baryons*, IAU Symp., 244, 300
- Greco, C., Dall’Ora, M., Clementini, G., et al. 2008, *ApJ*, 675, L73
- Hartwick, F. D. A. 2000, *AJ*, 119, 2248
- Hernandez, X., Mendosa, S., Suarez, T., & Bernal, T. 2010, *A&A*, 514, A101
- Hunter, D. A., Hunsberger, S. D., & Roye, E. W. 2000, *ApJ*, 542, 137
- Ibata, R., Chapman, S., Irwin, M., Lewis, G., & Martin, N. 2006, *MNRAS*, 373, L70
- Jerjen, H. 2010, *Adv. Astron.*, 2010, 1
- Jerjen, H., Kalnajs, A., & Binggeli, B. 2000, *A&A*, 358, 845
- Kallivayalil, N., van der Marel, R. P., & Alcock, C. 2006, *ApJ*, 652, 1213
- Karachentsev, I. D., Karachentseva, V. E., & Sharina, M. E. 2005, in *Near-fields cosmology with dwarf elliptical galaxies*, ed. H. Jerjen, & B. Binggeli, IAU Coll., 198, 295
- Kazantzidis, S., Mayer, L., Mastropietro, C., et al. 2004, *ApJ*, 608, 663
- Kent, S. M. 1989, *AJ*, 97, 1614
- Kirby, E. N., Guhathakurta, P., Bullock, J. S., et al. 2009, *Astro2010: The Astronomy and Astrophysics Decadal Survey*, Science White Papers, 156
- Klessen, R. S., & Kroupa, P. 1998, *ApJ*, 498, 143
- Klimentowski, J., Lokas, E. L., Knebe, A., et al. 2010, *MNRAS*, 402, 1899
- Klypin, A., Kravtsov, A. V., Valenzuela, O., & Prada, F. 1999, *ApJ*, 522, 82
- Koch, A., & Grebel, E. K. 2006, *AJ*, 131, 1405
- Koch, A., Wilkinson, M. I., Kleyna, J. T., et al. 2009, *ApJ*, 690, 453
- Kochanek, C. S., & Schechter, P. L. 2004, *Measuring and Modeling the Universe*, 117
- Kollmeier, J. A., Gould, A., Shectman, S., et al. 2009, *ApJ*, 705, L158
- Komatsu, E., Dunkley, J., Nolta, M. R., et al. 2009, *ApJS*, 180, 330
- Koposov, S. E., Yoo, J., Rix, H.-W., et al. 2009, *ApJ*, 696, 2179
- Knebe, A., Arnold, B., Power, C., & Gibson, B. K. 2008, *MNRAS*, 386, 1029
- Kroupa, P. 1997, *New Astron.*, 2, 139
- Kroupa, P., Theis, C., & Boily, C. M. 2005, *A&A*, 431, 517
- Kruijssen, J. M. D., & Mieske, S. 2009, *A&A*, 500, 785
- Kruijssen, J. M. D., & Lamers, H. J. G. L. M. 2008, *A&A*, 490, 151
- Kuehn, C., Kinemuchi, K., Ripepi, V., et al. 2008, *ApJ*, 674, L81
- Kuhn, J. R. 1993, *ApJ*, 409, L13
- Kuhn, J. R., & Miller, R. H. 1989, *ApJ*, 341, L41
- Kuhn, J. R., Smith, H. A., & Hawley, S. L. 1996, *ApJ*, 469, L93
- Kunkel, W. E. 1979, *ApJ*, 228, 718
- Law, D. R., & Majewski, S. R. 2010, *ApJ*, 714, 229
- Law, D. R., Majewski, S. R., & Johnston, K. V. 2009, *ApJ*, 703, L67
- Lee, J., & Komatsu, E. 2010, *ApJ*, 718, 60
- Li, Y.-S., & Helmi, A. 2008, *MNRAS*, 385, 1365
- Li, Y.-S., De Lucia, G., & Helmi, A. 2010, *MNRAS*, 401, 2036
- Libeskind, N. I., Frenk, C. S., Cole, S., Jenkins, A., & Helly, J. C. 2009, *MNRAS*, 399, 550
- Lisker, T. 2009, *Astron. Nachr.*, 330, 1043
- Lynden-Bell, D. 1976, *MNRAS*, 174, 695
- Lynden-Bell, D. 1983, in *Internal Kinematics and Dynamics of Galaxies*, ed. E. Athanassoula, IAU Symp., 100, 89
- Lynden-Bell, D., & Lynden-Bell, R. M. 1995, *MNRAS*, 275, 429
- Macciò, A. V., & Fontanot, F. 2010, *MNRAS*, 404, L16
- Macciò, A. V., Dutton, A. A., van den Bosch, F. C., et al. 2007, *MNRAS*, 378, 55
- Macciò, A. V., Kang, X., & Moore, B. 2009, *ApJ*, 692, L109
- Macciò, A. V., Kang, X., Fontanot, F., et al. 2010, *MNRAS*, 402, 1995
- Mainini, R., Macciò, A. V., Bonometto, S. A., & Klypin, A. 2003, *ApJ*, 599, 24
- Martin, N. F., Coleman, M. G., De Jong, J. T. A., et al. 2008a, *ApJ*, 672, L13
- Martin, N. F., de Jong, J. T. A., & Rix, H.-W. 2008b, *ApJ*, 684, 1075
- Mastropietro, C., & Burkert, A. 2008, *MNRAS*, 389, 967
- Mateo, M. L. 1998, *ARA&A*, 36, 435

- Mateo, M., Olszewski, E. W., Pryor, C., et al. 1993, *AJ*, 105, 510
- McGaugh, S. 2010, *AIP Conf. Ser.*, 1240, 13
- McGaugh, S. S. 2004, *ApJ*, 609, 652
- McGaugh, S. S. 2005a, *Phys. Rev. Lett.*, 95, 171302
- McGaugh, S. S. 2005b, *ApJ*, 632, 859
- McGaugh, S. S. 2008, *ApJ*, 683, 137
- McGaugh, S. S., & Wolf, J. 2010, *ApJ*, 722, 248
- McGaugh, S. S., de Blok, W. J. G., Schombert, J. M., Kuzio de Naray, R., & Kim, J. H. 2007, *ApJ*, 659, 149
- Metz, M. 2008, Ph.D. Thesis, University of Bonn
- Metz, M., & Kroupa, P. 2007, *MNRAS*, 376, 387
- Metz, M., Kroupa, P., & Jerjen, H. 2007, *MNRAS*, 374, 1125
- Metz, M., Kroupa, P., & Libeskind, N. I. 2008, *ApJ*, 680, 287
- Metz, M., Kroupa, P., & Jerjen, H. 2009a *MNRAS*, 394, 2223
- Metz, M., Kroupa, P., Theis, C., Hensler, G., & Jerjen, H. 2009b, *ApJ*, 697, 269
- Mieske, S., & Kroupa, P. 2008, *ApJ*, 677, 276
- Milgrom, M. 1983, *ApJ*, 270, 365
- Milgrom, M. 1995, *ApJ*, 455, 439
- Milgrom, M. 1999, *Phys. Lett. A*, 253, 273
- Milgrom, M. 2007, *ApJ*, 667, L45
- Milgrom, M. 2009a, *MNRAS*, 398, 1023
- Milgrom, M. 2009b, *Phys. Rev. D*, 80, 123536
- Milgrom, M. 2010, *MNRAS*, 403, 886
- Moffat, J. W. 2006, *J. Cosmol. Astro-Part. Phys.*, 3, 4
- Moffat, J. W., & Toth, V. T. 2008, *ApJ*, 680, 1158
- Moffat, J. W., & Toth, V. T. 2009a, *MNRAS*, L203
- Moffat, J. W., & Toth, V. T. 2009b, *Class. Quant. Grav.*, 26, 085002
- Moore, B., Ghigna, S., Governato, F., et al. 1999a, *ApJ*, 524, L19
- Moore, B., Diemand, J., Madau, P., Zemp, M., & Stadel, J. 2006, *MNRAS*, 368, 563
- Moretti, M. I., Dall'Orta, M., Ripepi, V., et al. 2009, *ApJ*, 699, L125
- Muñoz, R. R., Carlin, J. L., Frinchaboy, P. M., et al. 2006, *ApJ*, 650, L51
- Muñoz, R. R., Geha, M., & Willman, B. 2010, *AJ*, 140, 138
- Murray, N. 2009, *ApJ*, 691, 946
- Musella, I., Ripepi, V., Clementini, G., et al. 2009, *ApJ*, 695, L83
- Navarro, J. F., Frenk, C. S., & White, S. D. M. 1997, *ApJ*, 490, 493
- Navarro, J. F., Ludlow, A., Springel, V., et al. 2010, *MNRAS*, 402, 21
- Niederste-Ostholt, M., Belokurov, V., Evans, N. W., et al. 2009, *MNRAS*, 398, 1771
- Nipoti, C., Ciotti, L., Binney, J., & Londrillo, P. 2008, *MNRAS*, 386, 2194
- Okamoto, S., Arimoto, N., Yamada, Y., & Onodera, M. 2008, *A&A*, 487, 103
- Okamoto, T., & Frenk, C. S. 2009, *MNRAS*, 399, L174
- Okamoto, T., Frenk, C. S., Jenkins, A., & Theuns, T. 2010, *MNRAS*, 658
- Okazaki, T., & Taniguchi, Y. 2000, *ApJ*, 543, 149
- Oort, J. H. 1932, *Bull. Astr. Inst. Neth.* VI, 249
- Ott, J., Walter, F., & Brinks, E. 2005, *MNRAS*, 358, 1453
- Parriott, J. R., & Bregman, J. N. 2008, *ApJ*, 681, 1215
- Pawlowski, M., Kroupa, P., Metz, M., & de Boer, K. S. 2010, *A&A*, submitted
- Peacock, J. A. 2003, *Royal Society of London Transactions Series A*, 361, 2479
- Peacock, J. A. 1999, *Cosmological Physics*, ed. J. A. Peacock (Cambridge, UK: Cambridge University Press), 704
- Peebles, P. J. E., & Nusser, A. 2010, *Nature*, 465, 565
- Peñarrubia, J., McConnachie, A. W., & Navarro, J. F. 2008, *ApJ*, 672, 904
- Perlmutter, S., Aldering, G., Goldhaber, G., et al. 1999, *ApJ*, 517, 565
- Pflamm-Altenburg, J., & Kroupa, P. 2009, *MNRAS*, 397, 488
- Pflamm-Altenburg, J., & Kroupa, P. 2009b, *ApJ*, 706, 516
- Press, W. H., Teukolsky, S. A., Vetterling, W. T., & Flannery, B. P. 1992, *Numerical recipes in C. The art of scientific computing*, 2nd edn. (Cambridge: Cambridge University Press)
- Primack, J. R. 2009, *AIP Conf. Ser.*, 1166, 3
- Presotto, V., Iovino, A., Pompei, E., & Tempurin, S. 2010, *A&A*, 510, A31
- Recchi, S., Theis, C., Kroupa, P., & Hensler, G. 2007, *A&A*, 470, L5
- Reyes, R., Mandelbaum, R., Seljak, U., et al. 2010, *Nature*, 464, 256
- Riess, A. G., Filippenko, A. V., Challis, P., et al. 1998, *AJ*, 116, 1009
- Rubin, V. C., & Ford, W. K. Jr. 1970, *ApJ*, 159, 379
- Sakamoto, T., & Hasegawa, T. 2006, *ApJ*, 653, L29
- Sand, D. J., Olszewski, E. W., Willman, B., et al. 2009, *ApJ*, 704, 898
- Sand, D. J., Seth, A., Olszewski, E. W., et al. 2010, *ApJ*, 718, 530
- Sanders, R. H. 1999, *ApJ*, 512, L23
- Sanders, R. H. 2005, *MNRAS*, 363, 459
- Sanders, R. H. 2007, *MNRAS*, 386, 1588
- Sanders, R. H. 2008, talk presented at XX Rencontres de Blois, *Astropar. Phys.*, eprint [arXiv:0806.2585]
- Sanders, R. H., & McGaugh, S. S. 2002, *ARA&A*, 40, 263
- Sanders, R. H., & Noordermeer, E. 2007, *MNRAS*, 379, 702
- Serra, A. L., Angus, G. W., & Diaferio, A. 2009 [arXiv:0907.3691]
- Shaya, E., Olling, R., Ricotti, M., et al. 2009, *Astro2010: The Astronomy and Astrophysics Decadal Survey*, *Science White Papers*, 274
- Siegel, M. H. 2006, *ApJ*, 649, L83
- Simon, J. D., & Geha, M. 2007, *ApJ*, 670, 313
- Skordis, C. 2009, *Class. Quant. Grav.*, 26, 143001
- Spergel, D. N., Bean, R., Dore, O., et al. 2007, *ApJS*, 170, 377
- Strigari, L. E., Bullock, J. S., Kaplinghat, M., et al. 2008, *Nature*, 454, 1096 (S08)
- Tegmark, M., Blanton, M. R., Strauss, M. A., et al. 2004, *ApJ*, 606, 702
- Tiret, O., & Combes, F. 2007, *A&A*, 464, 517
- Tiret, O., & Combes, F. 2008, in *ASP Conf. Ser.*, 396, ed. J. G. Funes, & E. M. Corsini, 259
- Tollerud, E. J., Bullock, J. S., Strigari, L. E., & Willman, B. 2008, *ApJ*, 688, 277
- Tully, R. B., & Fisher, J. R. 1977, *A&A*, 54, 661
- Unruh, W. G. 1975, *Phys. Rev. D*, 14, 870
- van den Bergh, S. 1999, *A&A Rev.*, 9, 273
- van den Bergh, S. 2008, *Nature*, 455, 1049
- van der Marel, R. P., Alves, D. R., Hardy, E., & Suntzeff, N. B. 2002, *AJ*, 124, 2639
- Walsh, S. M., Jerjen, H., & Willman, B. 2007, *ApJ*, 662, L83
- Walsh, S. M., Willman, B., Sand, D., et al. 2008, *ApJ*, 688, 245
- Walsh, S. M., Willman, B., & Jerjen, H. 2009, *AJ*, 137, 450
- Watkins, L. L., Evans, N. W., Belokurov, V., et al. 2009, *MNRAS*, 398, 1757
- Weidner, C., Kroupa, P., & Larsen, S. S. 2004, *MNRAS*, 350, 1503
- Weil, M. L., Eke, V. R., & Efsthathiou, G. 1998, *MNRAS*, 300, 773
- Wetzstein, M., Naab, T., & Burkert, A. 2007, *MNRAS*, 375, 805
- Willman, B., Blanton, M. R., West, A. A., et al. 2005a, *AJ*, 129, 2692
- Willman, B., Dalcanton, J. J., Martinez-Delgado, D., et al. 2005b, *ApJ*, 626, L85
- Wolf, J., Martinez, G. D., Bullock, J. S., et al. 2010, *MNRAS*, 406, 1220
- Zhao, H. S. 1996, *MNRAS*, 283, 149
- Zhao, H. S. 2008, *J. Phys. Conf. Ser.*, 140, 012002
- Zhao, H., & Famaey, B. 2010, *Phys. Rev. D*, 81, 087304
- Zlosnik, T., Ferreira, P., & Starkman, G. 2007, *Phys. Rev. D*, 75, 044017
- Zucker, D. B., Belokurov, V., Evans, N. W., et al. 2006a, *ApJ*, 643, L103
- Zucker, D. B., Belokurov, V., Evans, N. W., et al. 2006b, *ApJ*, 650, L41
- Zwicky, F. 1933, *Helvetica Physica Acta*, 6, 110
- Zwicky, F. 1937, *ApJ*, 86, 217
- Zwicky, F. 1956, *ErNW*, 29, 344